Bulletin of Engineering Geology and the Environment (2021) 80:6473–6495
https://doi.org/10.1007/s10064-021-02307-1

ORIGINAL PAPER

Microseismic zonation maps for Egypt using shear wave velocity (V_s 30), and standard penetration resistance value (N_{30})

Mohamed A. Gamal[1] · **Mahmoud Elhussein**[1]

Received: 17 February 2021 / Accepted: 24 May 2021 / Published online: 31 May 2021

Abstract

Although Egypt has not been subjected to high seismic hazards, it does face a very high level of risk on this front. Even a small earthquake of moderate magnitude, such as the Faiyum earthquake of 1992 (Ms = 5.2), may turn into a catastrophic event causing collapse of or irreparable damage to thousands of buildings. This vulnerability is due to the country's lack of seismic site classifications and bad engineering conditions of buildings, especially in villages. A total of 71 drilling boreholes and about 82 shear wave seismic velocity tests varying between the Downhole, Crosshole, Refraction Microtremors (ReMi), and Multichannel Analysis Surface Waves (MASW) methods were used to prepare the microseismic zonation maps for Egypt. Microseismic zonation maps were introduced using the geological map of Egypt, NEHRP Seismic site classifications based on "shear wave velocity" (V_s 30), and the "soil refusal depth map" (SPT (N_{30}) = 50). Furthermore, new empirical equations to obtain V_s 30 versus SPT (N_{30}) were introduced to help engineers and seismologists obtain the desired dynamic properties of the soil, such as the dynamic shear modulus (G). The seismic activities inside the Egyptian plate were combined with the microseismic zonation maps to analyze the important seismic hazards; this was done for variable soils. The present study is expected to be a regional reference for the expected shear wave velocity, SPT (N_{30}) value, and shear rigidity constant for the different Egyptian soils and to help in the developing projects.

Keywords SPT · NEHRP · Shear wave velocity · N_{30} · Seismic hazard · Egypt

Introduction

Egypt is one of the very few countries in the world that is subjected to different seismotectonic activities. The seismicity of Egypt is mainly controlled by the active opening or the Red Sea rift on its the eastern boundary (Freund 1970; Girdler and Styles 1974; Cochran 1983; Girdler 1985), subduction in the Mediterranean Sea on the northern boundary (McKenzie 1972; Papazachos and Comninakis 1971; Quennell 1984; Papazachos et al. 1993), and some seismotectonic provinces inside the Egyptian plateau such as Faiyum, Aswan, and Abu Debbab (Kebeasy 1990; Woodword Clyde Consultant 1985).

After the disastrous 1992 earthquake (Ms = 5.2), Egypt came to be considered a high-risk country for earthquake activities. As a result, a new earthquake network for strong motions (acceleration and velocity) was installed by the National Research Institute of Astronomy and Geophysics.

Shear wave seismic velocity (V_s) is a very important measure for determining the site response of earthquake energy. It may even be considered the basic parameter that defines the dynamic properties of soils. It is very useful in the evaluation of soil stiffness, rigidity, hardness, strength, and liquefaction potential or foundation settlements (Richart et al. 1970; Seed and Idriss 1970; Schnabel et al. 1972; Walter 1981; Sykora and Stokoe 1983; Burland 1989; Sasitharan et al. 1994; Shibuya et al. 1995; Kramer 1996; Andrus and Stokoe 1997; Wills and Silva 1998; Mayne et al. 1999; Dobry et al. 2000; Lehane and Fahey 2002; Seed et al. 2003; Stewart et al. 2003; McGillivray and Mayne 2004; Idriss and Boulanger 2004; Holzer et al. 2005; McGillivray 2007; Akin et al. 2011; Cavallaro et al. 2018; Grasso et al. 2021).

We can say that earthquake resistance design, soil structure interaction, soil amplification, and damping depend on the Dynamic shear modulus (G) or on shear wave seismic velocity (V_s) and density (ρ) of the underlying soil.

✉ Mahmoud Elhussein
mahmoudelnouishy@yahoo.com

[1] Department of Geophysics, Faculty of Science, Cairo University, P.O. 12613, Giza, Egypt

$$G = \rho V_s^2. \quad (1)$$

Many studies have been carried out to determine the empirical relations for V_s soils (Ohba and Toriumi 1970; Imai and Yoshimura 1970; Fujiwara 1972; Ohsaki and Iwasaki 1973; Imai 1977; Ohta and Goto 1978; Seed and Idriss 1981; Imai and Tonouchi 1982; Sykora and Stokoe 1983; Jinan 1987; Lee 1990; Sisman 1995; Iyisan 1996; Kayabalı 1996; Jafari et al. 1997, 2002; Pitilakis et al. 1999; Kiku et al. 2001; Andrus et al. 2006; Hasançebi and Ulusay 2007; Hanumantharao and Ramana 2008; Dikmen 2009; Castelli et al. 2018).

Microseismic zonation map provides the basis for site-specific risk analysis, which can help in the mitigation of earthquake damage such as building collapses and liquefaction of soil and estimation of other response of soil layers under earthquake excitations (Grasso and Maugeri 2009, 2012). It can be used for evaluating site-specific risk analysis, which is essential for critical structures like nuclear power plants, subways, bridges, elevated highways, sky trains, and dam sites.

In this study, two site specific equations were deduced for each geological zone, one for V_s/depth variation and the other for N_{30}/depth variation. As it is very difficult to obtain the values of V_s and SPT (N_{30}) simultaneously at the same depth level, the empirical relations between V_s and SPT (N_{30}) were not calculated directly. They were calculated by solving the two equations of V_s and SPT (N_{30}) together as they are both function of depth. The collected data shows good quality, and this appears in the similarity of the V_s and SPT (N_{30}) slopes with depth for the same zones. The site-specific equations for V_s/D or SPT (N_{30})/D and hence V_s/SPT (N_{30}) are expected to serve as a reference for new developing projects in Egypt.

Brief description of seismotectonic provinces in egypt

The tectonics and seismotectonics of Egypt are a result of the interaction between three major tectonic plates: African, Eurasian, and European. A summary of the active seismic source zones in Egypt is given below. Figure 1 provides an illustration of these zones.

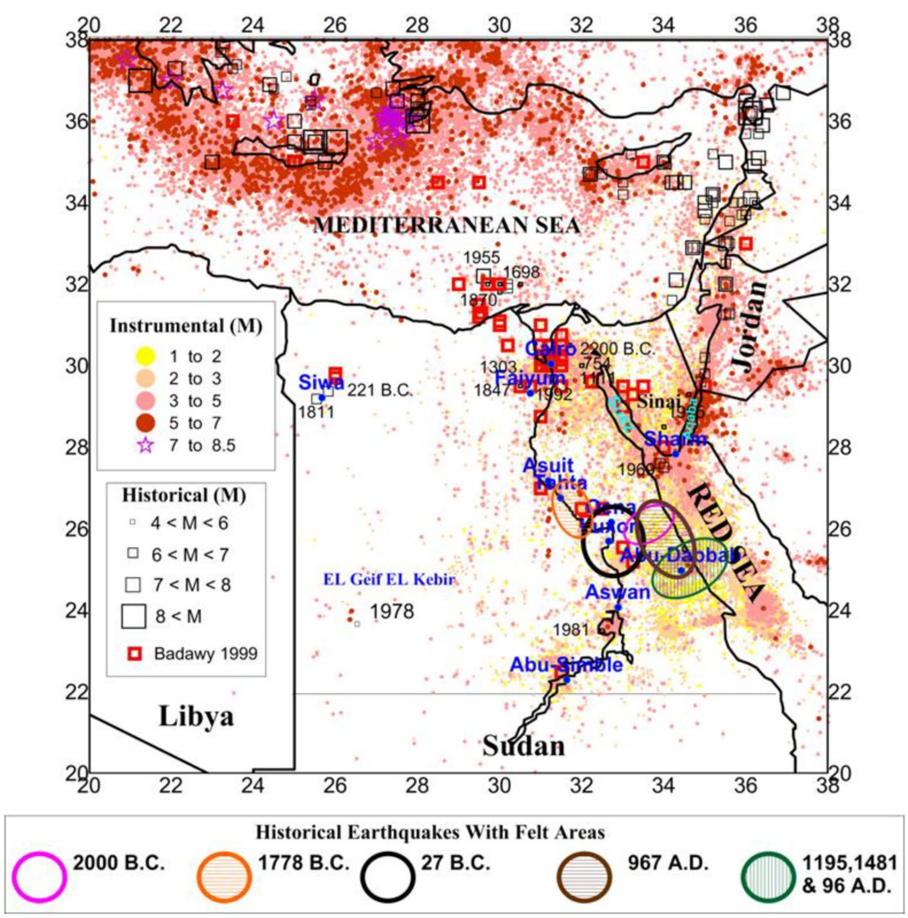

Fig. 1 Instrumental and historical earthquakes affecting Egypt from 2200 B.C. to 2020 from different sources. Some historical earthquakes are put with felt areas. The dates of some of the important earthquakes are written beside its earthquakes (integrated from Makropoulos and Burton 1981; Maamoun et al. 1984; Ben-Menahem 1979; Woodward-Clyde Consultants 1985; Riad and Meyers 1985; Shapira 1994; NEIC and USGS 1964–2020)

Subduction in the mediterranean sea (northern boundary)

The African lithosphere is subducting underneath the European lithosphere in the Hellenic Arc beneath Cyprus and the Crete Islands (McKenzie 1972; Papazachos and Comninakis 1971; Quennell 1984; Papazachos et al. 1993). This source produces the biggest earthquakes, with magnitudes that can reach Ms = 8. However, this zone is relatively far from urban areas in Egypt (Fig. 1).

Obduction in the red sea (eastern boundary)

The opening of the Red Sea is separated on two motions. These are a transform motion at the Gulf of Aqaba-Levant transform fault system and an opening of the Gulf of Suez (Freund 1970; Girdler and Styles 1974; Cochran 1983; Girdler 1985). This seismic source produces relatively large earthquakes that can reach Ms = 7 and affect certain urban areas in Egypt like east Cairo (Egypt's capital), Sinai, and the Red Sea zone east of Egypt.

Some active seismotectonic provinces (within the egyptian plate)

These are some geographical regions inside the Egyptian plate that are known for producing seismic activities but for tectonic reasons that are not yet well understood. Some of these active seismic trends are the "Suez-Cairo-Alexandria" trend, the Pelusium trends (East of Cairo and Faiyum), Aswan, and the Abu Debbab area (Maamoun et al. 1984; Neev 1982; Kebeasy 1990; Meshref 1990).

The seismic sources from these zones produce moderate earthquakes of magnitude Ms = 3–6; however, they are potentially the most destructive seismic sources affecting Egypt because of their vicinity to crowded cities like Cairo, Faiyum, and Aswan.

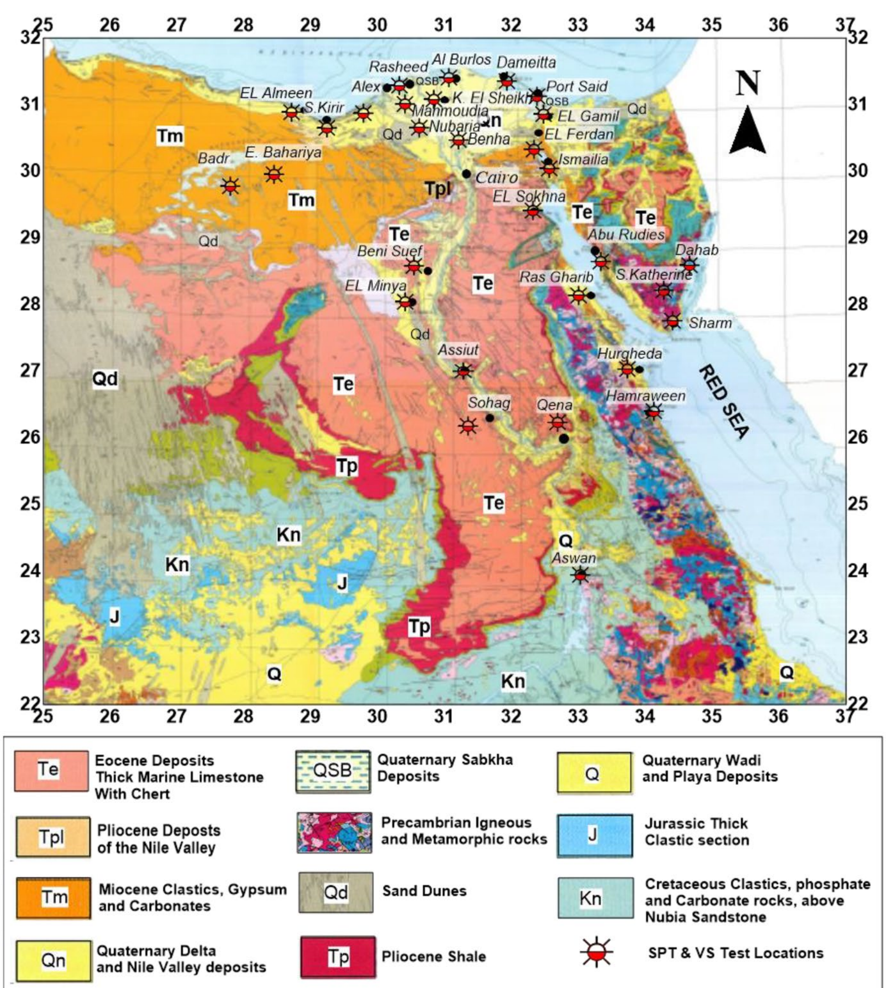

Fig. 2 Geological map of Egypt (modified from EGSMA, 1981) showing the locations of the 26 test sites for both V_s and SPT (N_{30}) values

Classification of geological zones

The following is a brief description of the geology of different zones in Egypt:

The eastern desert

The Eastern Desert is bound to the west by the Nile. The western part of Eastern Desert is covered by Cretaceous sandstone and the north by Eocene limestone and then Miocene clastics (EGSMA 1981) (Fig. 2). The desert is mainly composed of igneous and metamorphic rocks dating back to the Precambrian age. The basement rocks found here include granite, gabbro, rhyolite, andesite, basalt, schist, slate, and gneisses. These rocks are covered by Quaternary deposits of sand and gravel, raised beaches, and Miocene covers of gypsum and carbonates.

The western desert

Most of the central part of the Western Desert is composed of thick Eocene marine limestone with minor clay beds. The depressions of Farafra and Bahariya are covered by Cretaceous limestones and layers of Paleocene shale, while the northern part has a Miocene age basal clastic section overlain by carbonate units. The southern part of the Western Desert is covered by Cretaceous sandstone (Nubia sandstone) and some Jurassic clastic rocks, and the south-east and east of the Western Desert are covered by Quaternary sand, forming the Great Sand Sea (EGSMA 1981) (Fig. 2).

The nile valley and delta

The Nile deposits consist of loose or semi-consolidated Quaternary sediments, sand, silt, clay, and gravel with several changes in deposition sequence due to the Nile's course changes over time. The Nile Delta is covered by cultivated lands of the Quaternary age. The Nile brachiates into two branches before it meets the Mediterranean Sea (Rashid and Damietta). A lot of sabkhas exist in these areas especially in the lagoon areas of Lake Bardawil, Lake Burulus, and Lake Manzala. The sabkha deposits are a very famous composition characterized by the existence of large layers of salt, clay, sand, silt, and sometimes organic matter (EGSMA 1981) (Fig. 2).

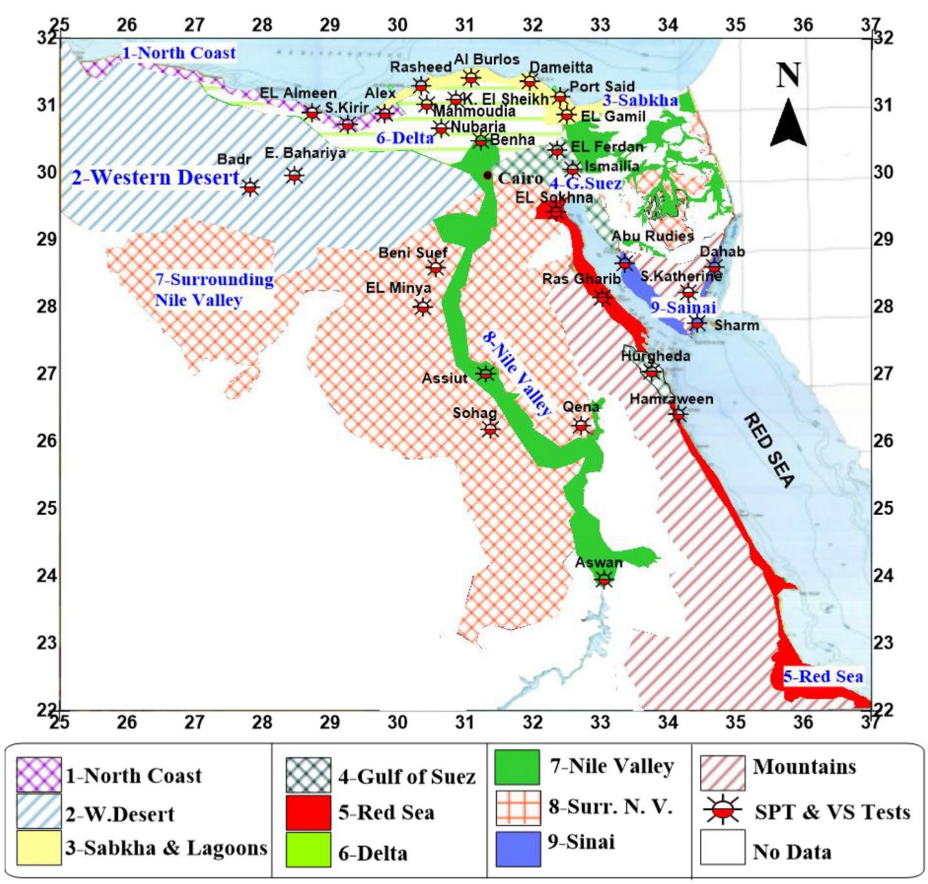

Fig. 3 The main geological zones classified for this study using the V_s and SPT data, namely, (1) The North Coast, (2) The Western Desert, (3) Sabkha and Lagoons, (4) The Gulf of Suez, (5) The Red Sea, (6) The Delta, (7) The Nile Valley, (8) The Surrounding Nile Valley, and (9) The Sinai Peninsula

Sinai

The Sinai Peninsula forms a portion of the Arabo-Nubian Shield and occupies a wedge-shaped block at the northern end of the East African Rift System, bound by the Gulf of Aqaba to the southeast and the Gulf of Suez to the southwest.

South Sinai is mainly composed of Precambrian igneous and metamorphic rocks caped by Quaternary wadi and Playa deposits, while in the north, it consists of sand dunes, Quaternary wadi and Playa deposits, Eocene beds of thick limestone, and/or Cretaceous fossiliferous clastics, with Jurassic coals around the Gabal Maghara. Most of the lowlands in the north and northeast are covered by Quaternary sand (EGSMA 1981) (Fig. 2).

Based on the regional geology and data collected from 26 sites as well as the Vs and SPT (N30) values, this study classified the following nine different geological zones: (1) the North Coast, (2) the Western Desert, (3) Sabkha and Lagoons, (4) the Gulf of Suez, (5) the Red Sea, (6) the Delta, (7) the Nile Valley, (8) the zone surrounding the Nile Valley, and (9) the Sinai Peninsula. About 71 drilling in-situ SPT (N30) value tests and about 82 Vs tests (Downhole, Crosshole, ReMi, or MASW) were used to introduce microseismic zonation maps for Egypt (Fig. 3).

Data collection and methodology

Standard penetration test (SPT) method

SPT is considered a high-strain in-situ test designed to provide information on the geotechnical engineering properties of the soil. This test uses a thick-walled sample tube driven into the ground (45 cm) by hammering blows on its top with a slide hammer. The first 15 cm are considered seating for the tube while the last 30 cm are recorded as the soil

Table 1 Locations of the V_s tests and the drilled boreholes for determining the SPT (N_{30}) values

Zone	Location	Shear wave tests	SPT BH logs	GWL
1-North Coast	Alexandria	6 downholes	6	3
	Sidi krir	2 downholes	———-	3
	Almeen	5 MASW	8	1.5
2-Western Desert	Badr	2 downholes	2	——-
	East Bahariya	2 downholes	2	——-
3-Sabkha and Lagoons	Rasheed	2 downholes	2	1
	Al Burlos	2 downholes	8	1.10
	Dameitta	3 downholes, 2 crossholes	1	1
	Port-Said	4 downholes	2	1
	ELGamil	2 downholes	2	0.6
4-Gulf of Suez	Ferdan	4 downholes	4	1.9
	Ismailia	3 downholes	2	11
	Hurghada	1 downhole	1	———
5-Red Sea	El Sokhna	1 downhole	4	20
	Ras Gharib	2 MASW	7	——
	Hamraween	2 downholes	2	12
6-Delta	Kafr El sheikh	7 downholes	7	1.7
	Mahmoudia	2 MASW	2	1.2
	Nubaria	2 downholes	———-	3
7-Surrounding Nile Valley	Beni Suef	1 REMI	———-	——
	El Minya	1 downhole	2	——
	Sohag	3 REMI	———-	——-
	Qena	2 downholes	2	——
8-Nile Valley	Benha	3 crossholes	———-	3
	Assuit	2 downholes	2	——-
	Aswan	3 downholes	3	——-
9-Sinai	Abu Rudies	5 MASW	———-	——-
	Sharm Elsheikh	1 downhole	———-	5
	Dahab	1 REMI	———-	——
	Saint Katherine	5 REMI	———-	——-

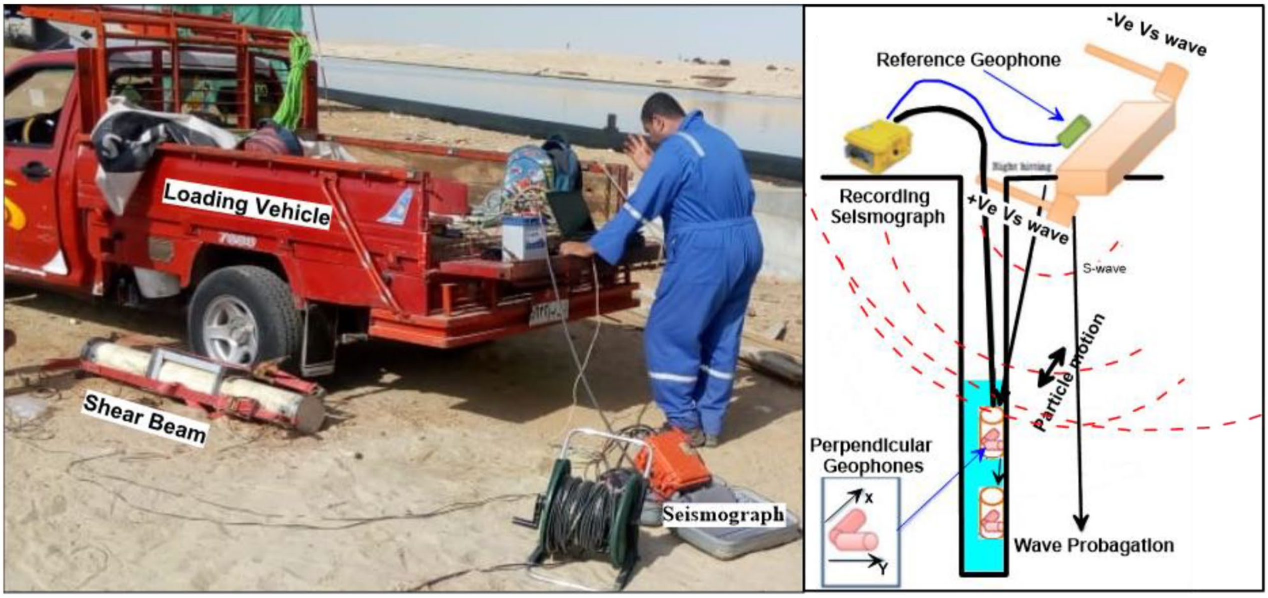

Fig. 4 Schematic diagram showing the downhole seismic test procedure used in this study (ASTM D7400 2017)

resistance value SPT (N30). If 50 blows are not sufficient to advance it through a 15-cm interval, the engineers consider this a refusal (ASTM D1586–99 1999). The V_s test is considered a low-strain test since it involves exciting the soil by sound to determine its dynamic properties by generally using a sledgehammer.

A total of 82 locations were chosen to account for all the geological variations in Egypt. About 71 boreholes were drilled, and 82 V_s tests were conducted varying between Downhole, Crosshole, ReMi, and MASW tests (Fig. 3 and Table 1). The depths of these boreholes ranged from 20 to 60 m. Undisturbed samples were taken at nearly 1-m depth

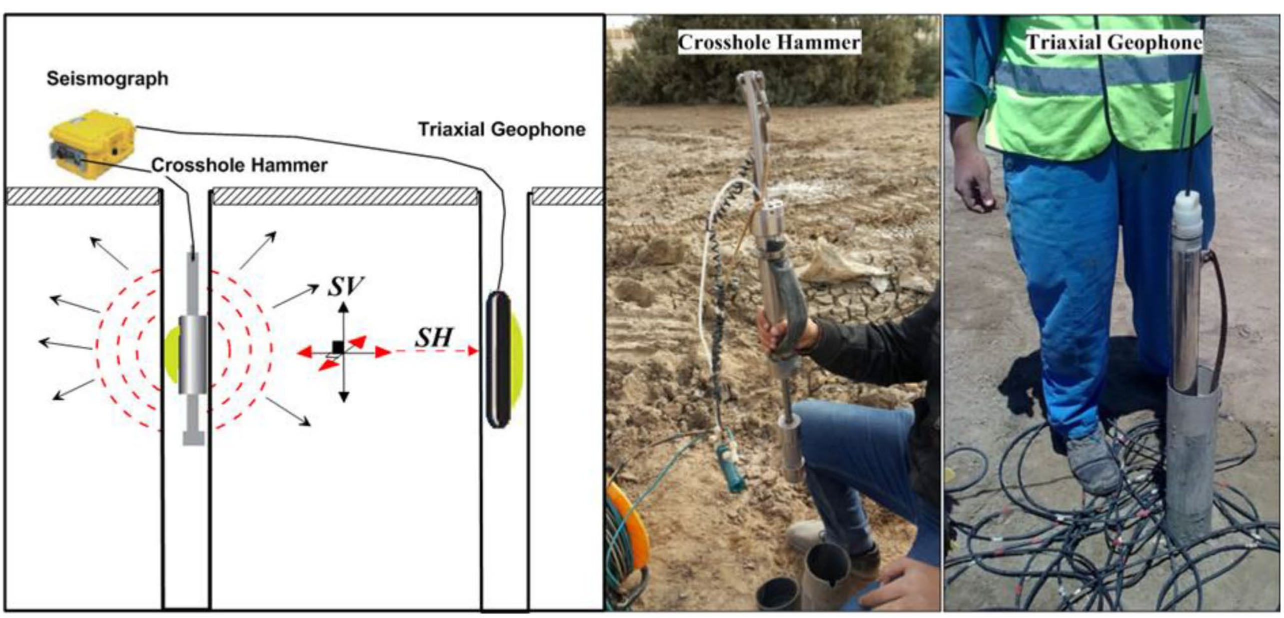

Fig. 5 Schematic diagram showing the Crosshole seismic test procedure used in this study (left). The Crosshole hammer source used (middle) and the 10HZ triaxial geophone (right; ASTM D4428 2014)

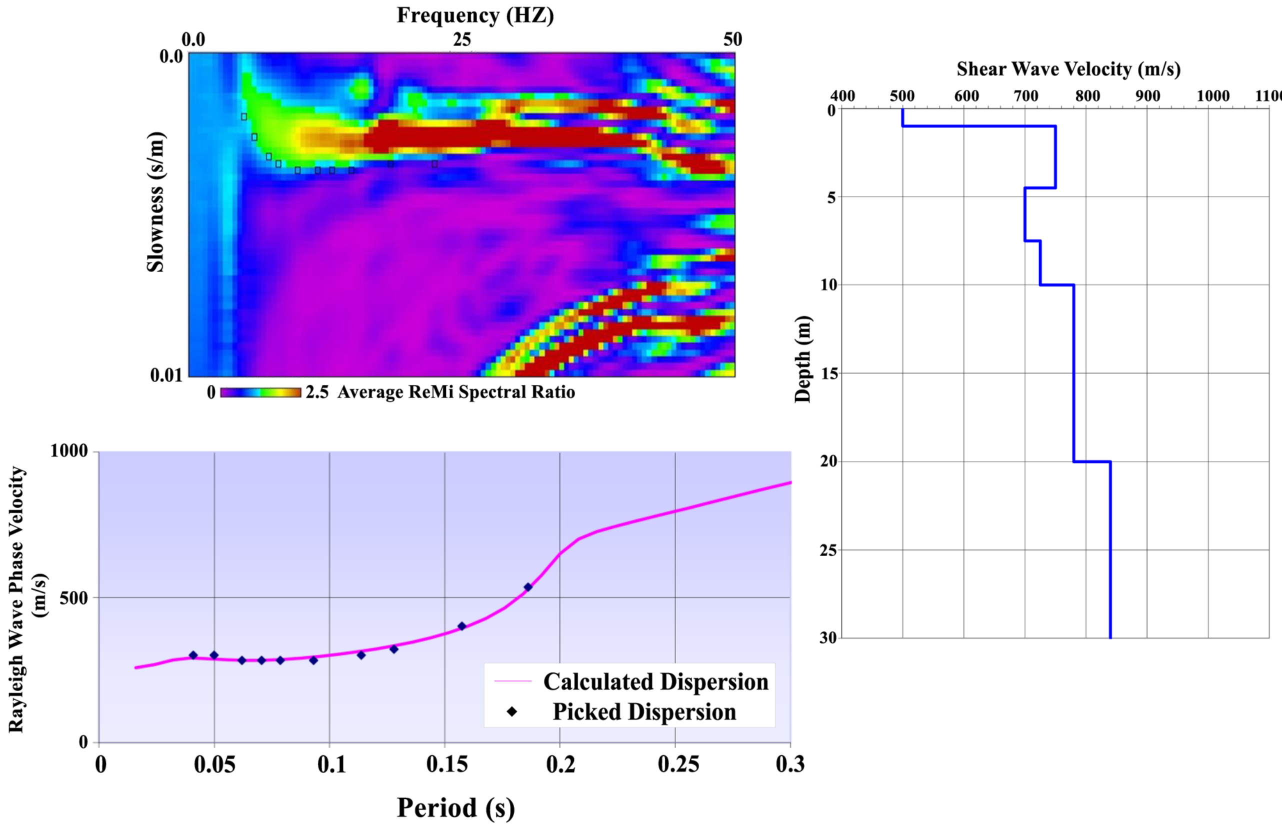

Fig. 6 Example of p-f image, dispersion curve excluded for the ReMi profile conducted at Sinai city (left) and corresponding V_s (right) (Louie 2001)

intervals, to obtain as continuous a soil profile as possible. Further, samples for the soil SPT blow counts were taken at 1-m depth intervals in most of the boreholes in the sandy layers. The ground water level for the studied areas varied between 1 and 20 m (Table 1) and is shown as encountered.

The following is a brief description of the tests used to determine the V_s.

Downhole seismic test method

A Downhole seismic test was conducted in this study with a three-component triaxial geophone 4HZ or 10 HZ (Vp, Vsh, and Vsz). The shear waves were generated using a wooden shear beam source of 15-cm diameter and 2.5-m length loaded by vehicle (Table 1 and Fig. 4). Both S + ve

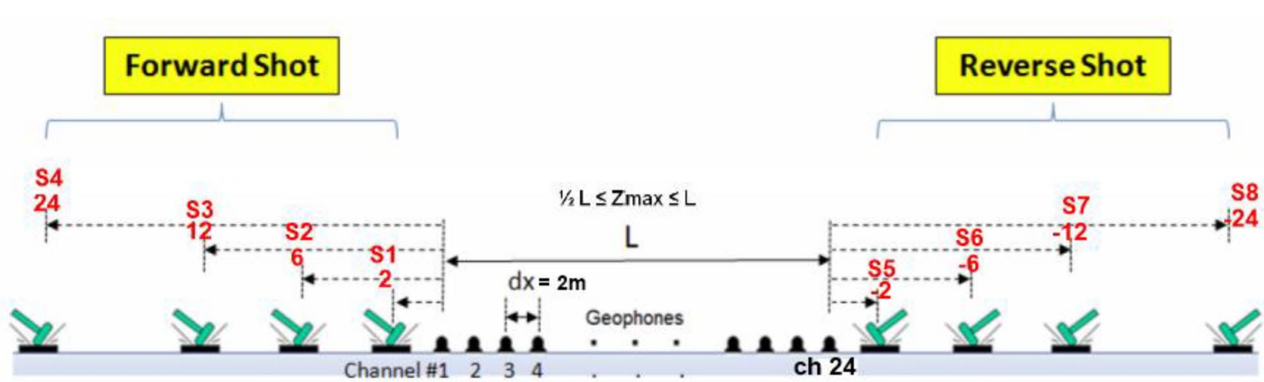

Fig. 7 Acquisition parameters used for MASW profiles for this study with 2–5-m geophone spacing and forward and reverse shots at 2, 6, 12, and 24–48 from both terminals of the profile

and S – ve shear waves were generated by opposite hitting on the wooden plate to generate the shear wave reversals (Fig. 4). The source used was a 10-kg impulsive hammer. The instruments used for this study were either the ES-3000 12 channel Geometrics, USA or the Geode 24 Channel from the same company (ASTM D7400 2017).

Crosshole seismic test method

A Crosshole seismic test was done using a shear wave seismic hammer placed inside the terminal borehole that was treated as the source borehole (ASTM D4428 2014) (Fig. 5). The seismic hammer was lowered to a certain depth. Thereafter, the two receiving geophones were lowered and located at the same depth using the cable connected to the geophones. Subsequently, a tension was applied to the clamps to achieve firm contact between the source, the geophones, and the borehole perimeter (Fig. 5).

The ReMi method

The ReMi method is a passive technique. It relies on the measurement of ambient noise carried out with linear seismic arrays to obtain information about the dispersion curve (V_s versus frequency) (Coccia et al. 2010). Practically, the ReMi method is based on a 2-D slowness-frequency (p-f) transformation of a microtremor record. This transformation separates the Rayleigh waves from other seismic waves (Gamal and Pullammanappallil 2011; Strobbia et al. 2015) (Fig. 6). The main advantages of using this technique accrue regardless of the triggered source and it works best with seismicity noise, e.g., traffic and different vehicles (Louie 2001; Pullammanappallil et al. 2003; Gamal and Pullammanappallil 2011). This method previously proved useful in estimating the average Vs for several sites in Egypt (Gamal and Pullammanappallil 2011). In this study, we have used this method several times for drilling boreholes, especially in remote areas like Sinai, but not for drilling a downhole or crosshole (Fig. 6 and Table 1).

The MASW method

The MASW technique (Park et al. 1999) has been used several times in this study (Table 1). It was developed in response to the shortcomings of the spectral analysis of surface wave method in the presence of noise. The simultaneous recording of 24 or more receivers at a short distance (2–5 m) was used with an impulsive or hammer source to measure the variation of V_s with depth (Fig. 7). The advantage of this method is that it provides a relatively greater depth of penetration that sometimes reaches half of the survey depth (Park et al. 1999; Miller et al. 2000) (Fig. 8).

Results and discussion

The following is a description of the data collected for each of the geological zones.

The north coast zone

This zone includes the cities of Alexandria, Almeen, and Sidikrir and represents the northern coast of Egypt. This zone is composed mainly of silty clay, silty sand, sandy clay,

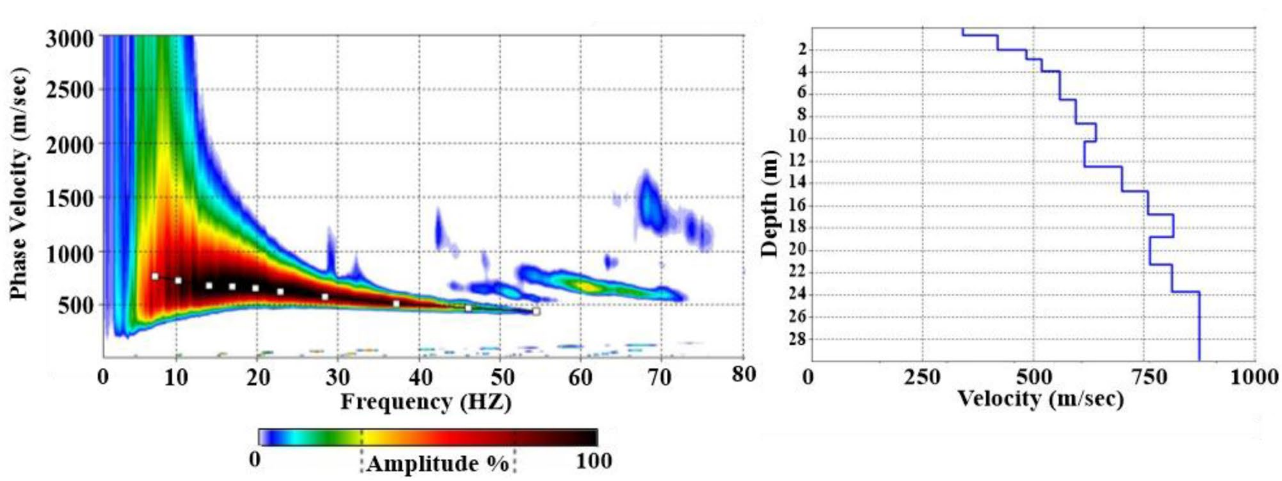

Fig. 8 Example of dispersion image and dispersion curve excluded for MASW profile conducted at Ras Gharib city (left) and corresponding V_s (right) (Park et al. 1999; Miller et al. 2000)

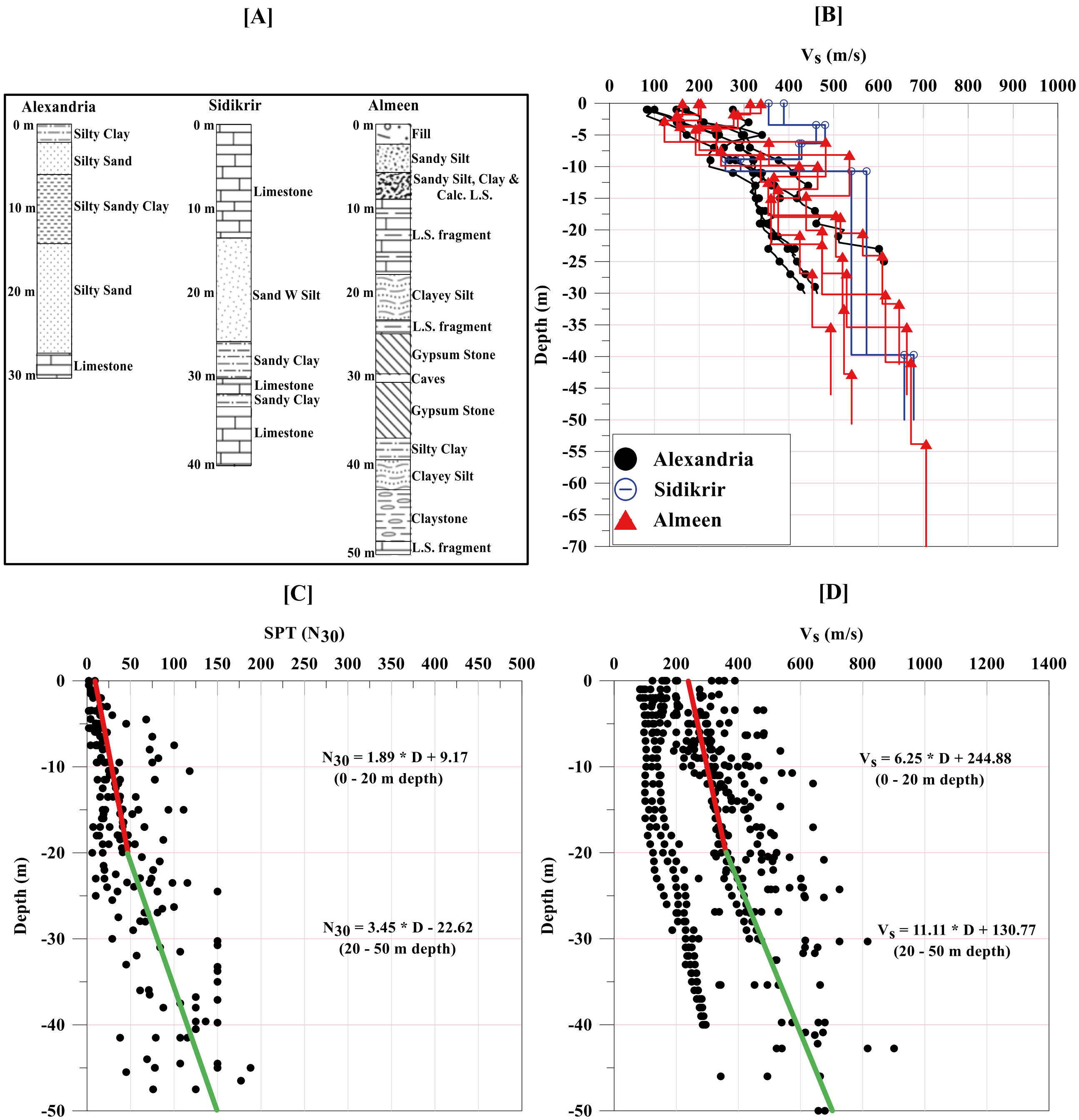

Fig. 9 Soil parameters for the North Coast zone. **A** Representative borehole logs, **B** V_s curves, **C** SPT (N_{30})/depth best-fit equations, and **D** velocity/depth best-fit equations

claystone, limestone fragments, gypsum stone, and limestone rock (Fig. 9A).

The original V_s curves are drawn in Fig. 9B. The entire SPT (N_{30}) data is illustrated in Fig. 9C and ranges from 10–150. The value of SPT (N_{30}) > 50 is calculated by extrapolation. Thus, for example, 50 blow counts driving the spoon 10 cm is converted into SPT (N_{30} cm) = 150. The entire data for V_s is illustrated in Fig. 9D and ranges from 220–600 m/s.

The SPT (N_{30})/depth best-fit equations and those for 0–20 m and 20–50 m are presented in Table 2 and Fig. 9C, while the velocity/depth best-fit equations and those for depths 0–20 m and 20–50 m are presented in Table 2 and Fig. 9D.

The western desert zone

This zone is represented by the cities of Badr and East Baheryа. This area is composed mainly of sand with silt and gravel, silty sand, and sand (Fig. 10A).

The original V_s curves are drawn in Fig. 10B. The entire SPT (N_{30}) data is illustrated in Fig. 10C and ranges from 50–150. The entire data for V_s is illustrated in Fig. 10D and ranges from 200–700 m/s.

The SPT (N_{30})/depth best-fit equations and those for 0–10 and 10–20 m are presented in Table 2 and Fig. 10C, while the velocity/depth best-fit equations and those for depths 0–10 m and 10–20 m are presented in Table 2 and Fig. 10D.

The sabkha and lagoon zone

This zone includes the cities of Rasheed, Al Burlos, Dameitta, Port Said, and El Gameil. It represents the sabkha and lagoon zones of Egypt. This area is composed mainly of silty sand, silty clay, sand with silt, sandy clay, and fat clay (Fig. 11A).

The original V_s curves are drawn in Fig. 11B. The entire SPT (N_{30}) data is illustrated in Fig. 11C and ranges from 3–150. The entire data for V_s is illustrated in Fig. 11D and ranges from 120–270 m/s.

The SPT N30/depth best-fit equations and those for 0–20 m and 20–60 m are presented in Table 2 and Fig. 11C, while the velocity/depth best-fit equations and those for depths 0–20 m and 20–60 m are presented in Table 2 and Fig. 11D.

The gulf of suez zone

This zone includes the cities of Ferdan, Hurgheda, and Ismailia. This zone is composed mainly of sand, sand with silt and gravel, sand with silt, sand traces, silt, traces of iron oxides, silty sand, sandy silt, clayey sand, silty clay, and thin layers of clay (Fig. 12A).

The original V_s curves are drawn in Fig. 12B. The entire SPT (N_{30}) data is illustrated in Fig. 12C and ranges from 25–150. The entire data for V_s is illustrated in Fig. 12D and ranges from 200–600 m/s.

The SPT (N_{30})/depth best-fit equations and those for 0–20 m and 20–40 m are presented in Table 2 and Fig. 12C, while the velocity/depth best-fit equations and those for depths 0–20 m and 20–40 m are presented in Table 2 and Fig. 12D.

The red sea zone

This zone is represented in our study by the cities of Hamraween, Elsokhna, and Ras-Gharieb, and this area is composed mainly of sand with gravel, sandstone with limestone, silty sand, sand with gravel, sandy silt, silty clay, fat clay, and gravel (Fig. 13A).

The original V_s curves are drawn in Fig. 13B. The entire SPT (N_{30}) data is illustrated in Fig. 13C and ranges from 25–150. The entire data for V_s is illustrated in Fig. 13D and ranges from 400–800 m/s.

The SPT (N30)/depth best-fit equations and those for 0–20 m and 20–40 m are presented in Table 2 and Fig. 13C,

Table 2 Best-fit equations for V_s versus the depth and standard penetration SPT (N_{30}) value versus the depth for different geological zones excluded from this study

Zone	Depth	Standard penetration value versus depth relation	Shear wave velocity versus depth relation
North Coast	0–20 m	$\mathbf{SPT\ (N_{30})} = 1.89 \times \mathbf{D} + 9.17$	$\mathbf{V_s} = 6.25 \times \mathbf{D} + 244.88$
	20–50 m	$\mathbf{SPT\ (N_{30})} = 3.45 \times \mathbf{D} - 22.62$	$\mathbf{V_s} = 11.11 \times \mathbf{D} + 130.77$
Western Desert	0–10 m	$\mathbf{SPT\ (N_{30})} = 7.69 \times \mathbf{D} + 42.38$	$\mathbf{V_s} = 33.33 \times \mathbf{D} + 162.67$
	10–20 m	$\mathbf{SPT\ (N_{30})} = 3.57 \times \mathbf{D} + 87.82$	$\mathbf{V_s} = 9.09 \times \mathbf{D} + 450.27$
Sabkha and Lagoon	0–20 m	$\mathbf{SPT\ (N_{30})} = 0.71 \times \mathbf{D} + 3.93$	$\mathbf{V_s} = 1.72 \times \mathbf{D} + 111.14$
	20–60 m	$\mathbf{SPT\ (N_{30})} = 4.35 \times \mathbf{D} - 68.65$	$\mathbf{V_s} = 3.13 \times \mathbf{D} + 85.06$
Gulf of Suez	0–20 m	$\mathbf{SPT\ (N_{30})} = 4.35 \times \mathbf{D} + 19.17$	$\mathbf{V_s} = 10 \times \mathbf{D} + 199.20$
	20–40 m	$\mathbf{SPT\ (N_{30})} = 1.79 \times \mathbf{D} + 72.29$	$\mathbf{V_s} = 3.23 \times \mathbf{D} + 329.84$
Red Sea	0–20 m	$\mathbf{SPT\ (N_{30})} = 3.57 \times \mathbf{D} + 27.29$	$\mathbf{V_s} = 14.56 \times \mathbf{D} + 420.84$
	20–40 m	$\mathbf{SPT\ (N_{30})} = 1.12 \times \mathbf{D} + 76.76$	$\mathbf{V_s} = 5.012 \times \mathbf{D} + 612.14$
Delta zone	0–20 m	$\mathbf{SPT\ (N_{30})} = 1.18 \times \mathbf{D} + 25.55$	$\mathbf{V_s} = 5 \times \mathbf{D} + 139.65$
	20–40 m	$\mathbf{SPT\ (N_{30})} = 0.61 \times \mathbf{D} + 37.06$	$\mathbf{V_s} = 3.13 \times \mathbf{D} + 171.22$
Surrounding Nile Valley	0–12.5 m	$\mathbf{SPT\ (N_{30})} = 5.88 \times \mathbf{D} + 47.71$	$\mathbf{V_s} = 50 \times \mathbf{D} + 230$
	12.5–40 m	$\mathbf{SPT\ (N_{30})} = 0.76 \times \mathbf{D} + 111.28$	$\mathbf{V_s} = 3.70 \times \mathbf{D} + 714.26$
Nile Valley	0–20 m	$\mathbf{SPT\ (N_{30})} = 0.95 \times \mathbf{D} + 38.30$	$\mathbf{V_s} = 7.14 \times \mathbf{D} + 146.29$
	20–40 m	$\mathbf{SPT\ (N_{30})} = 2.94 \times \mathbf{D} - 2.18$	$\mathbf{V_s} = 11.11 \times \mathbf{D} + 62.22$

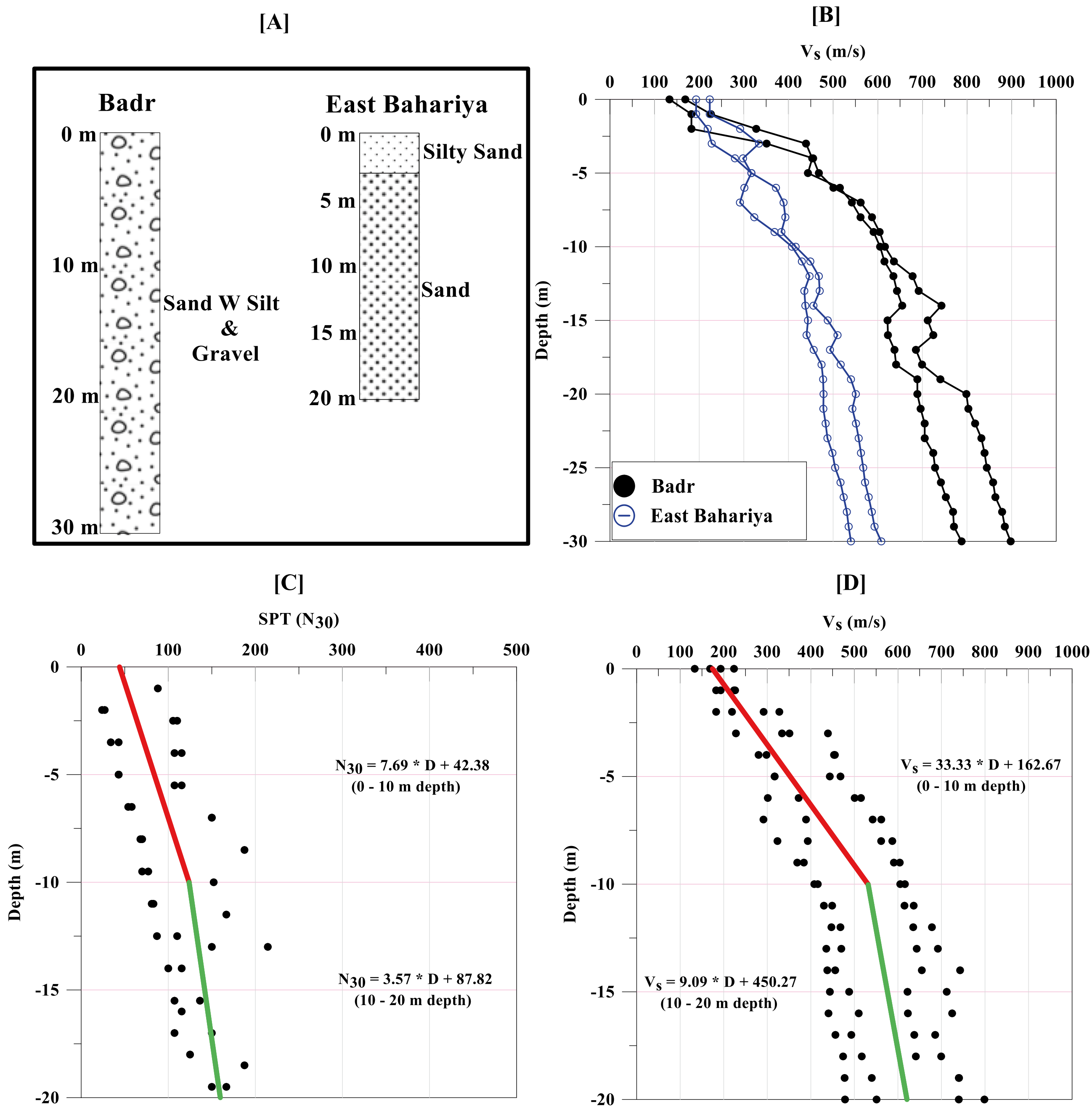

Fig. 10 Soil parameters for the Western Desert zone. **A** Representative borehole logs, **B** V_s curves, **C** SPT (N_{30})/depth best-fit equations, and **D** velocity/depth best-fit equations

while the velocity/depth best-fit equations and those for depths 0–20 m and 20–40 m are presented in Table 2 and Fig. 13D.

The delta zone

This zone is composed mainly of fat clay, silty sand, and sand with silt and is represented in this study by the Kafr El Sheikh, Mahmoudia, and Nubaria cities (Fig. 14A).

The original V_s curves are drawn in Fig. 14B. The entire SPT (N_{30}) data is illustrated in Fig. 14C and ranges from 25–100. The entire data for V_s is illustrated in Fig. 14D and ranges from 150–350 m/s.

The SPT (N_{30})/depth best-fit equations and those for 0–20 m and 20–40 m are presented in Table 2 and Fig. 14C, while the velocity/depth best-fit equations and those for depths 0–20 m and 20–40 m are listed in Table 2 and Fig. 14D.

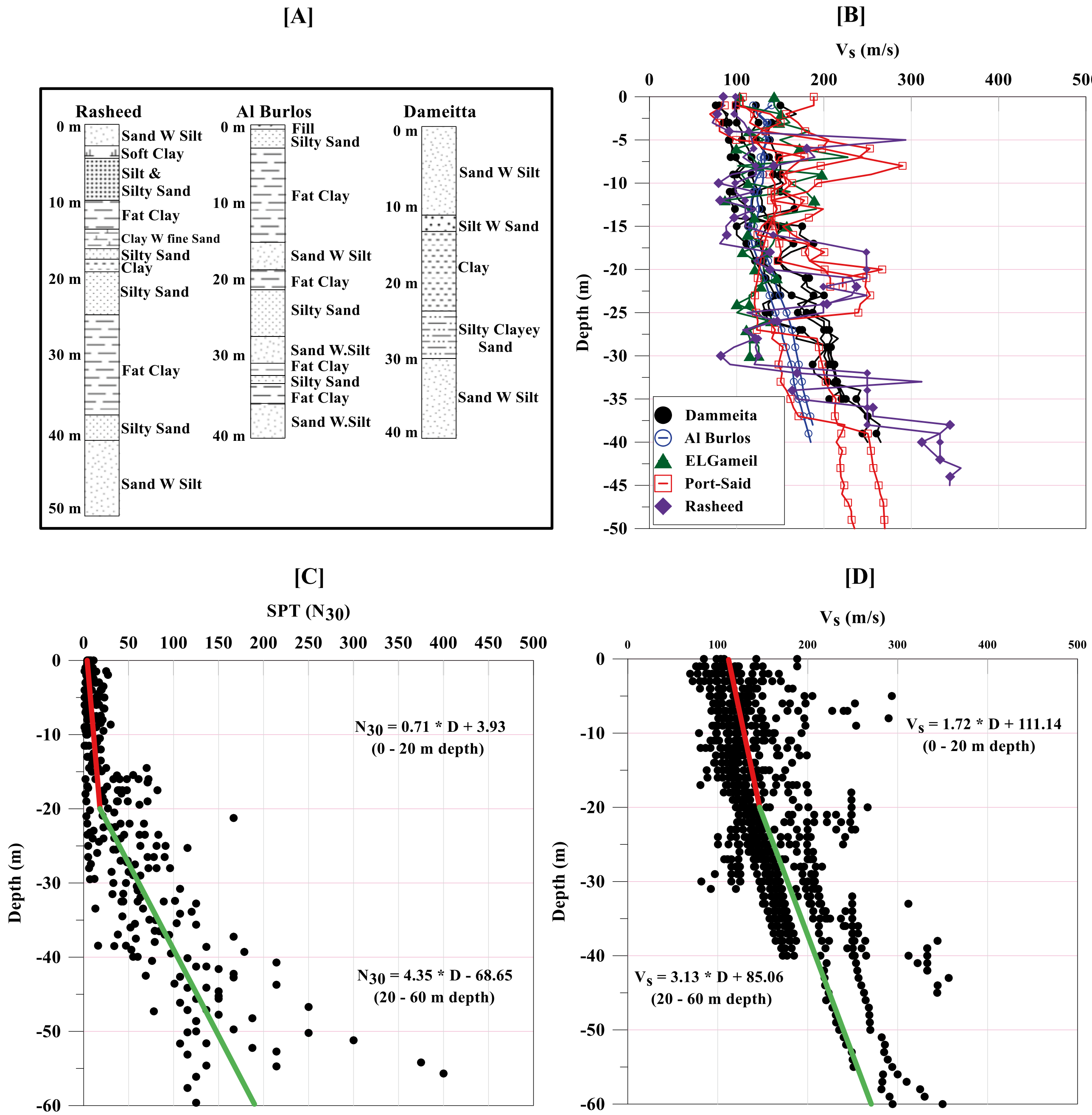

Fig. 11 Soil parameters for the Sabkha and Lagoons zone. **A** Representative borehole logs, **B** V_s curves, **C** SPT (N_{30})/depth best-fit equations, and **D** velocity/depth best-fit equations

The zone surrounding the nile valley

The zone surrounding the Nile Valley is represented in this study by the cities of Quena, Sohag, Elmenya, and Beni Suef. This zone is composed mainly of silty clay, claystone, siltstone, cemented sand, sand, dolomite limestone, crystalline limestone, silty sand with gravel, siliceous limestone, and gravel (Fig. 15A).

The original V_s curves are drawn in Fig. 15B. The entire SPT (N_{30}) data is illustrated in Fig. 15C and ranges from 50–200. The entire data for V_s is illustrated in Fig. 15D and ranges from 200–900 m/s.

The SPT (N_{30})/depth best-fit equations and those for 0–12.5 m and 12.5–40 m are listed in Table 2 and Fig. 15C, while the velocity/depth best-fit equations for depths 0–12.5 m and 12.5–40 m are listed in Table 2 and Fig. 15D.

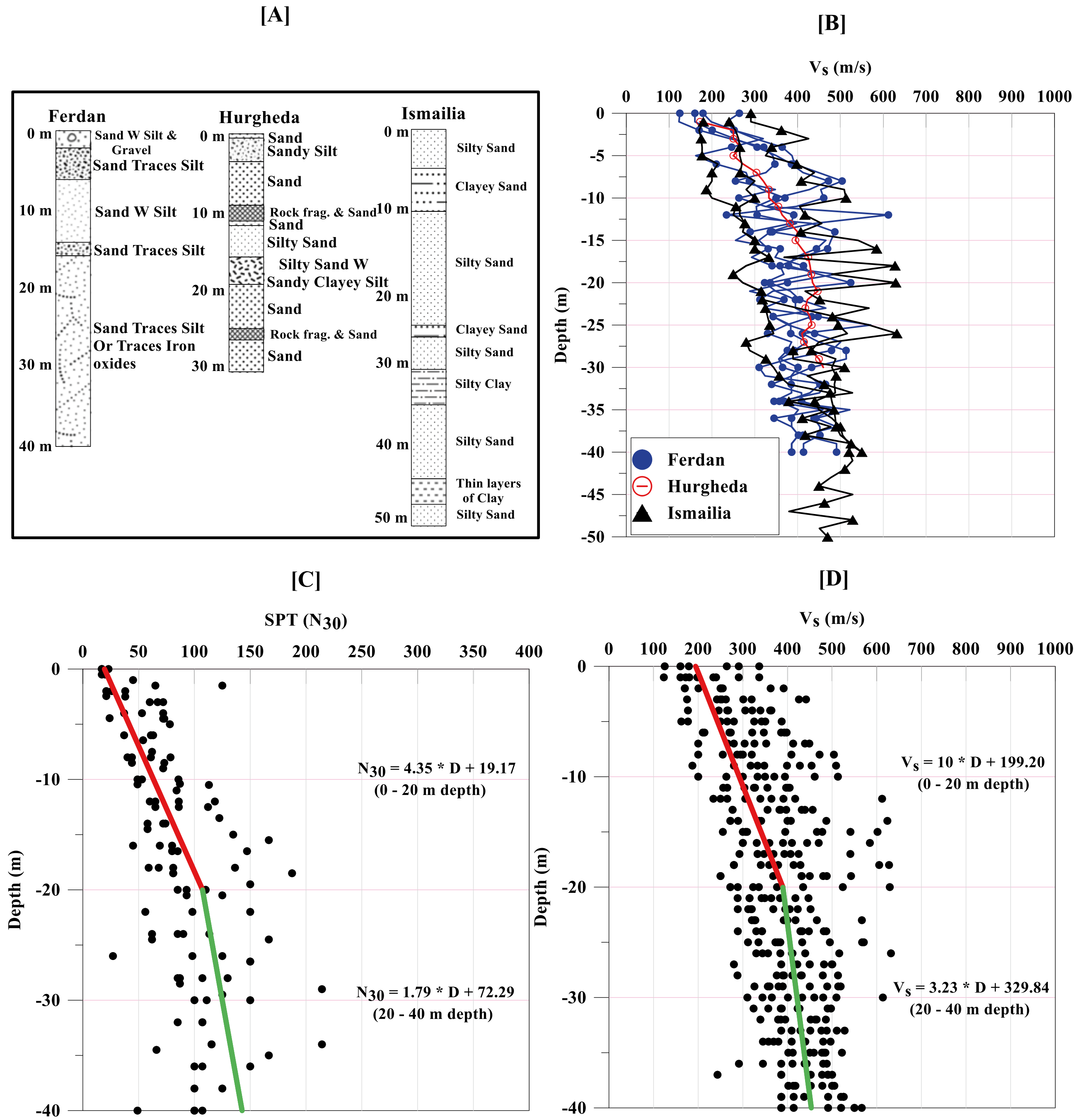

Fig. 12 Soil parameters for the Gulf of Suez zone. **A** Representative borehole logs, **B** V_s curves, **C** SPT (N_{30})/depth best-fit equations, and **D** velocity/depth best-fit equations

The nile valley zone

The Nile Valley zone is represented by the cities of Assuit, Aswan, and Benha. This zone is composed mainly of silty clay, silty sand, sand and sand with silt, and gravel (Fig. 16A).

The original V_s curves are drawn in Fig. 16B. The entire SPT (N_{30}) data is drawn in Fig. 16C and ranges from 40–120. The entire data for V_s is drawn in Fig. 16D and ranges from 120–600 m/s.

The SPT (N_{30})/depth best-fit equations and those for 0–20 m and 20–40 m are presented in Table 2 and Fig. 16C, while the velocity/depth best-fit equations for depths 0–20 m and 20–40 m are presented in Table 2 and Fig. 16D.

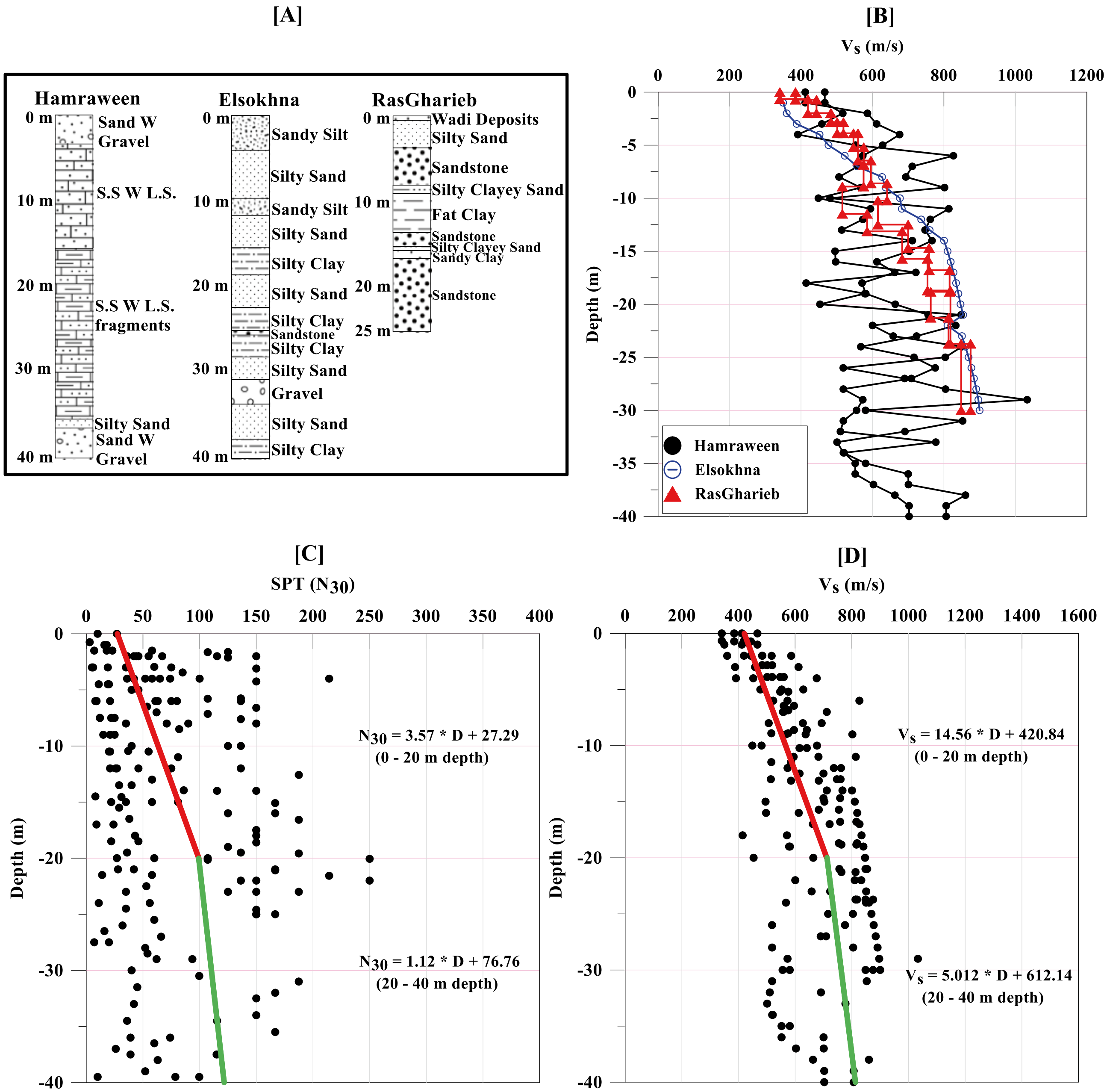

Fig. 13 Soil parameters for the Red Sea zone. **A** Representative borehole logs, **B** V_s curves, **C** SPT (N_{30})/depth best-fit equations, and **D** velocity/depth best-fit equations

Relations between V_s and SPT (N_{30})

The SPT (N_{30}) for the previously mentioned zones were compared with their corresponding V_s values to estimate the empirical relations between the V_s and SPT (N_{30}) for the different soil zones. These relations were estimated using the following steps:

a) Plot the SPT (N_{30}) versus the depth (D) for different zones (Figs. 9C–16C).
b) Plot the V_s versus the same range of D used in step (a) for the same locations and zones (Figs. 9D–16D).
c) Calculate the best-fit equations for V_s versus D and SPT (N_{30}) versus D.
d) As D is the same for both the equations, by solving both equations we can get the relation between V_s and SPT (N_{30}) for the different soil zones as can be seen in Table 3.

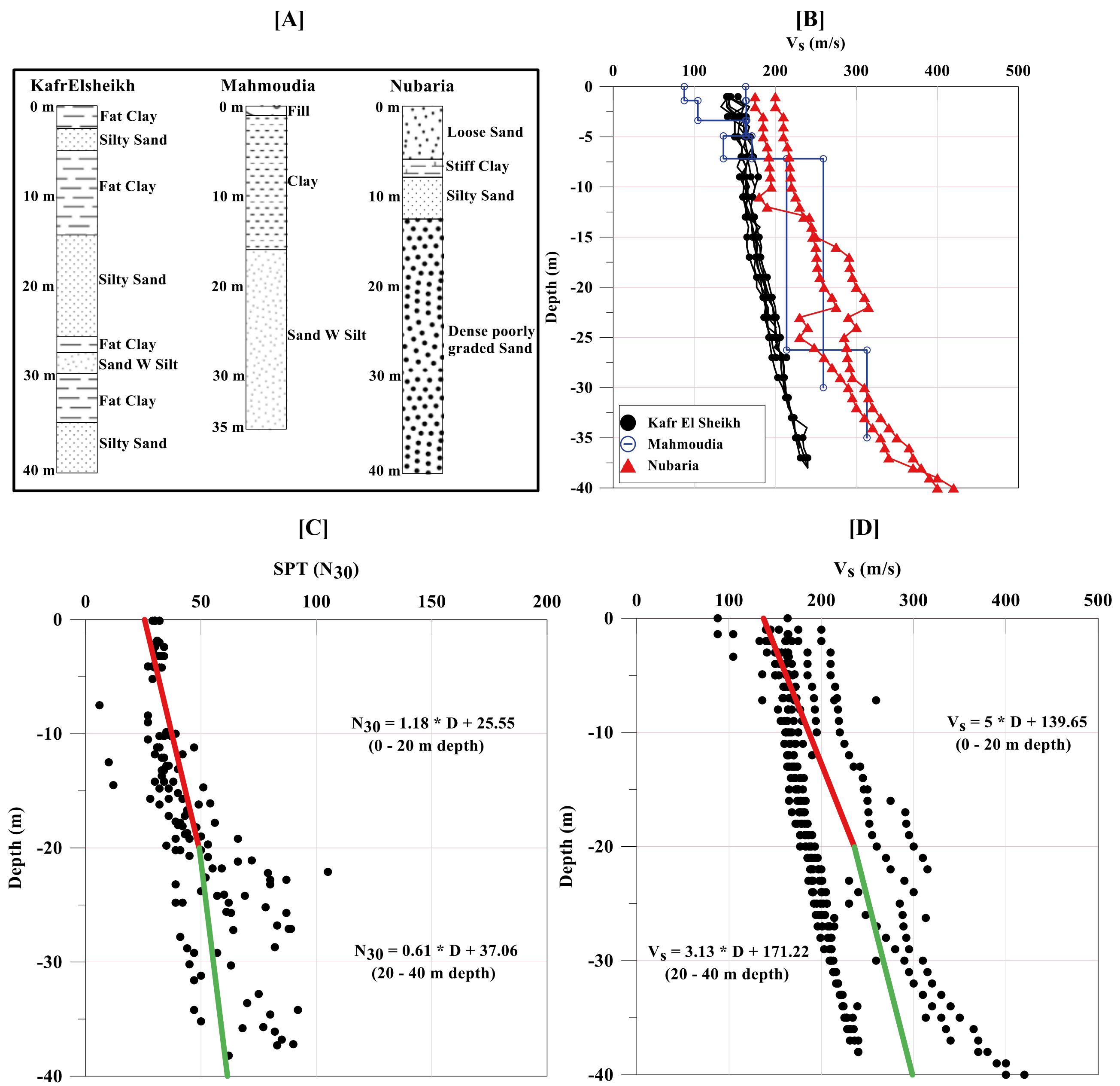

Fig. 14 Soil parameters for the Delta zone. **A** Representative borehole logs, **B** V_s curves, **C** SPT (N_{30})/depth best-fit equations, and **D** velocity/depth best-fit equations

The obtained relations are then compared with the different existing sources to show their consistency with these other sources (Kanai 1966; Imai and Yoshimura 1970; Ohba and Toriumi 1970; Fujiwara 1972; Ohsaki and Iwasaki 1973; Imai et al. 1975; Ohta and Goto 1978; Imai and Tonouchi 1982; Jinan 1987; Yokota et al. 1991; Athanasopoulos 1995; Sisman 1995; Kiku et al. 2001; Jafari et al. 2002; Hasançebi and Ulusay 2007; Hanumantharao and Ramana 2008; Dikmen 2009). This comparison has been shown in Fig. 17.

Microseismic zonation maps for Egypt based on NEHRP (V_s 30) and refusal depth SPT(N_{30})

Two important microseismic seismological quantities were introduced for this study in one map. These quantities were the V_s for the upper 30 m and the refusal depth map for the upper 50 m. The V_s 30 was calculated for the different Egyptian soil zones using the following equation (Kanlı et al. 2006):

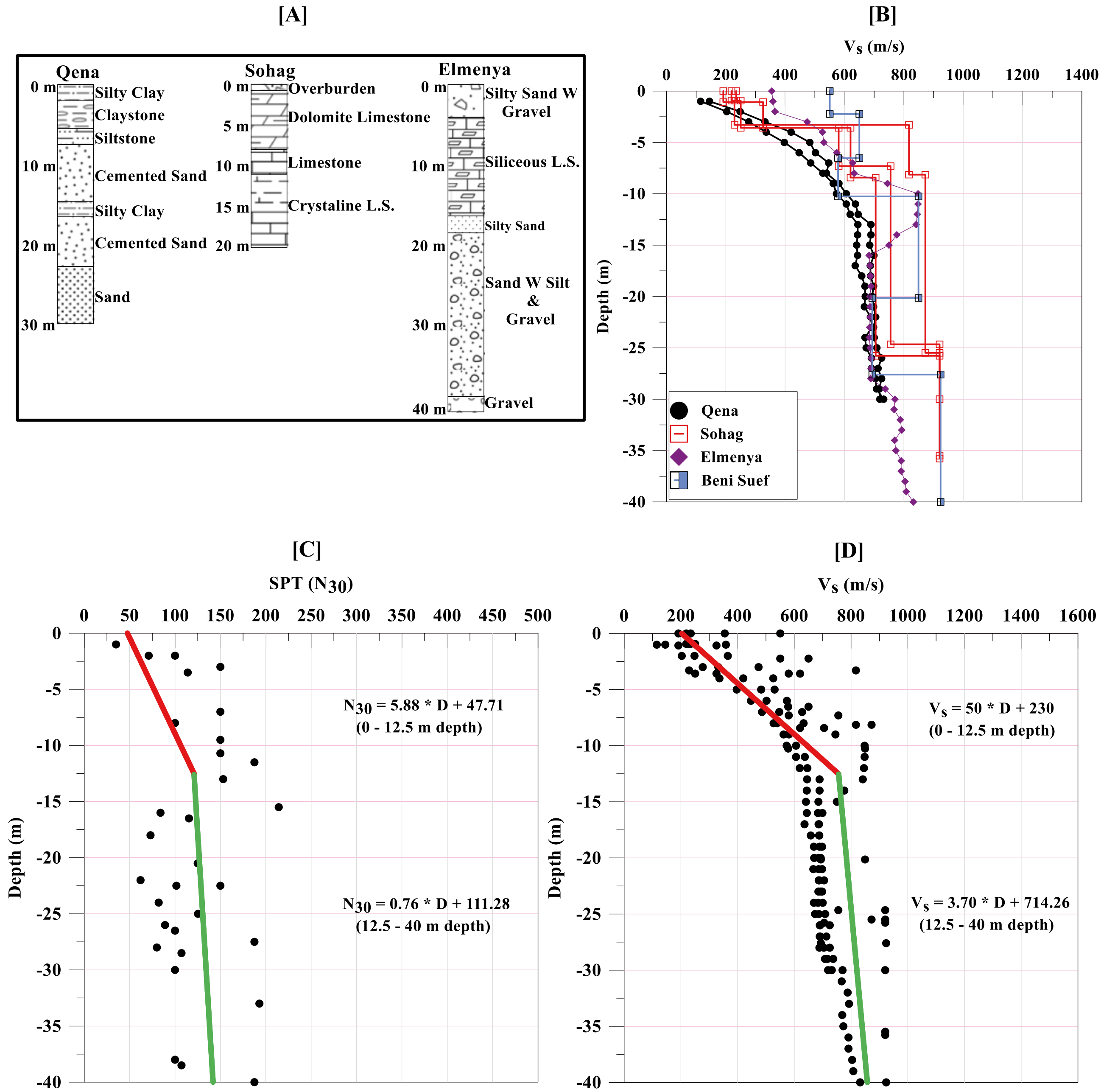

Fig. 15 Soil parameters for the surrounding Nile Valley zone. **A** Representative borehole logs, **B** V_s curves, **C** SPT (N_{30})/depth best-fit equations, and **D** velocity/depth best-fit equations

$$V_s 30 = \frac{30}{\sum \left(\frac{d_i}{V_{s_i}} \right)} \quad (2)$$

where d_i is the thickness of layer i and V_{s_i} is the shear wave velocity of layer i. The V_s 30 is calculated for the different soil zones and a V_s 30 map for the different Egyptian soils is produced from these calculations (Fig. 18).

To produce the refusal depth map for different Egyptian soils (D50 map), we have used the depth at which the spoon penetrates 30 cm inside the soil after producing 50 blows (SPT (N_{30}) = 50) or D50 as referred to on the map (Fig. 18). This was done using the SPT (N_{30}) versus (D) equations for each of the zones given in Table 2. These different depths for different Egyptian soil zones were used to produce an SPT (N_{30}) D50 map of the different

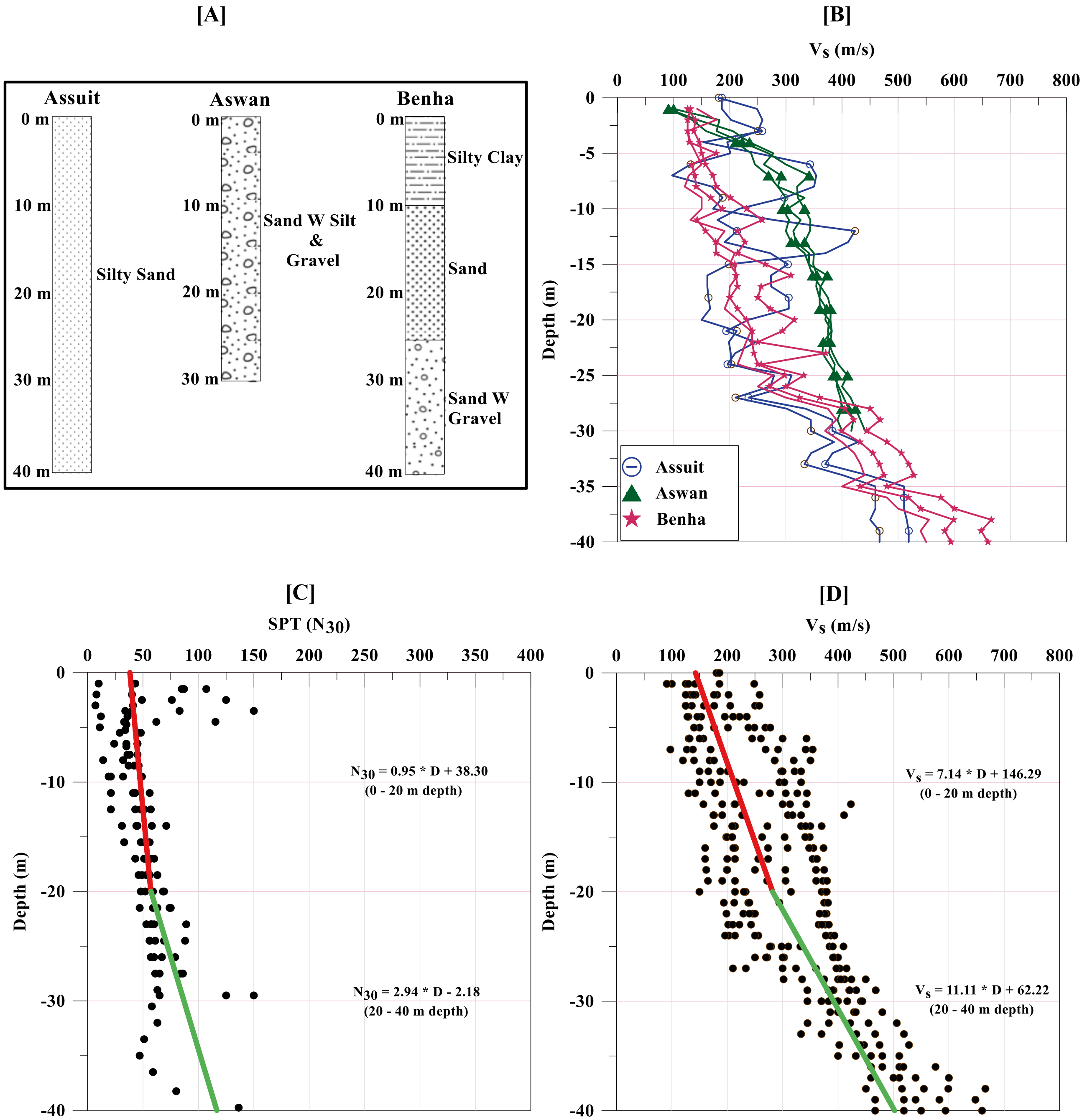

Fig. 16 Soil parameters for the Nile Valley zone. **A** Representative borehole logs, **B** V_s curves, **C** SPT (N_{30})/depth best-fit equations, and **D** velocity/depth best-fit equations

Egyptian soils, which is a function of the strength of the soil (Fig. 18).

The NEHRP/(V_s 30) seismic site classification was then used to determine the soil classes for the different Egyptian soils. The different Egyptian soils were then arranged from weak to strong using the NEHRP (2007) classification and refusal depth (D50) as shown in Fig. 18 and Table 4.

The V_s calculated for the mountains at Saint Katherine area was used for the mountains of the Red Sea (Fig. 18). The general trend that can be seen from the microseismic zonation map is that of an increase in the V_s 30 as the strength of the soil increases, and a simultaneous decrease in the refusal depth except in the northern coast zone that is affected by the weak soil of the EL Almeen site. This site is affected by the presence of cavities, which make the soil here extremely weak (Fig. 9A).

Detection of seismic risk and warnings

This microseismic zonation map is the first attempt at a seismic hazard assessment of Egypt's soils (to the best of our knowledge). A regional assessment for the extent of hazard is believed to be very helpful for any new project to be taken up in Egypt. With the help of this map, we can get information about the NEHRP zone's classification, the V_s 30 value, and know the strength of the soil in terms of the SPT (N_{30}) refusal depth D50 (Fig. 18). However, in this regard, there are three important warnings for the people and decision-makers of Egypt:

1) Warning for the people in the weakest zone of "sabkha and lagoons":

   This zone is classified as zone "E" by the NEHRP seismic classification and is composed of soft clayey soil. The V_s detected in this zone is 133 m/s, while the refusal depth for SPT (N_{30}) is very deep at about 28 m (Fig. 18). Unfortunately, this zone has been seismically active since 1698 A.D. (Fig. 1). The seismic activities that caused the earthquakes of 1870 and 1955 were located offshore, under the sea. During the 1955 earthquake (Ms = 6.2; maximum intensity = VIII (Woodward and Clyde Consultant 1985)), 22 lives were lost, and many were injured. The weak soil in this zone, especially in Rashid and Idku, caused more than 300 buildings to be damaged. There was damage to infrastructure as well as pipelines to a large extent. Hence, a warning is given for this zone as many big projects and petroleum sector investments such as the liquefaction of natural gas in Rashid and Idku are being initiated in this zone.

Table 3 V_s SPT (N_{30}) relations for different soil zones in Egypt

Zone	Depth	Relation
North Coast	0–20 m	$V_s = 3.31 \times SPT(N_{30}) + 214.53$
	20–50 m	$V_s = 3.22 \times SPT(N_{30}) + 203.61$
Western Desert	0–10 m	$V_s = 4.33 \times SPT(N_{30}) - 21$
	10–20 m	$V_s = 2.55 \times SPT(N_{30}) + 226.73$
Sabkha and Lagoon	0–20 m	$V_s = 2.43 \times SPT(N_{30}) + 101.72$
	20–60 m	$V_s = 0.72 \times SPT(N_{30}) + 134.44$
Gulf of Suez	0–20 m	$V_s = 2.30 \times SPT(N_{30}) + 155.13$
	20–40 m	$V_s = 1.81 \times SPT(N_{30}) + 199.29$
Red Sea	0–20 m	$V_s = 4.08 \times SPT(N_{30}) + 309.54$
	20–40 m	$V_s = 4.48 \times SPT(N_{30}) + 268.64$
Delta zone	0–20 m	$V_s = 4.24 \times SPT(N_{30}) + 31.39$
	20–40 m	$V_s = 5.13 \times SPT(N_{30}) - 18.94$
Surrounding Nile Valley	0–12.5 m	$V_s = 7.52 \times SPT(N_{30}) - 141.56$
	12.5–40 m	$V_s = 3.78 \times SPT(N_{30}) + 70.46$
Nile Valley	0–20 m	$V_s = 7.52 \times SPT(N_{30}) - 141.56$
	20–40 m	$V_s = 3.78 \times SPT(N_{30}) + 70.46$

Fig. 17 Example showing the consistency of the obtained equations for the SPT (N_{30}) versus V_s with different sources (Kanai 1966; Imai and Yoshimura 1970; Ohba and Toriumi 1970; Fujiwara 1972; Ohsaki and Iwasaki 1973; Imai et al. 1975; Ohta and Goto 1978; Imai and Tonouchi 1982; Jinan 1987; Yokota et al. 1991; Athanasopoulos 1995; Sisman 1995; Kiku et al. 2001; Jafari et al. 2002; Hasançebi and Ulusay 2007; Hanumantharao and Ramana 2008; Dikmen 2009). **A** The Delta zone, **B** the Gulf of Suez zone, **C** the North Coast zone, and **D** the Red Sea zone

2) Warning for the people living in the "Delta Zone and the Capital Cairo":

   It became evident that the eastern part of Cairo and the Delta are active seismic zones that have experienced historical earthquakes that date back to 2200 B.C. (Fig. 1). The main reason for these activities is most probably the opening of the Gulf of Suez (Ben Menahem and Aboodi 1971). This area has the second weakest soil based on the V_s and NEHRP code (195 m/s and Zone "D") (Fig. 18). This is most probably due to the accumulation of the alluvium deposits of the Nile inside the Nile Valley and the Delta (Fig. 18). The main hazard in this area is manmade and arises from the existence of a lot of houses with failed engineering. These houses have been documented to be a reason for loss of life after intermediate earthquakes because of the soil and non-engineering constructions, especially ceilings made of wood. The intermediate earthquakes such as the Faiyum earthquake of 1992 (M = 5.8) caused the death of hundreds of people and damaged hundreds of houses. This destruction has always occurred in the case of the old brick houses built in villages and non-engineering houses built in Cairo, particularly those in the Dowiqa area (Woodward and Clyde Consultant 1985).

3) Warning for the people living in the Villages of the Nile Valley:

   The Nile Valley zone is the third weakest zone in Egypt, most probably due to the weak alluvium deposits of the Nile valley from Cairo to Aswan (Fig. 18). This zone possesses V_s of 232 m/s and is classified as NEHRP zone D. This zone consists of poor villages as well as many old brick and non-engineering houses. This zone has been affected by several earthquakes that have been documented since 27 B.C. The "High Dam" in Aswan, which is one of the most important strategic constructions, also exists in this zone. Hence, care should be taken to warn the people living in this zone. The future projects in this zone should also be duly warned given this zone's relative weakness compared to other geological zones in Egypt.

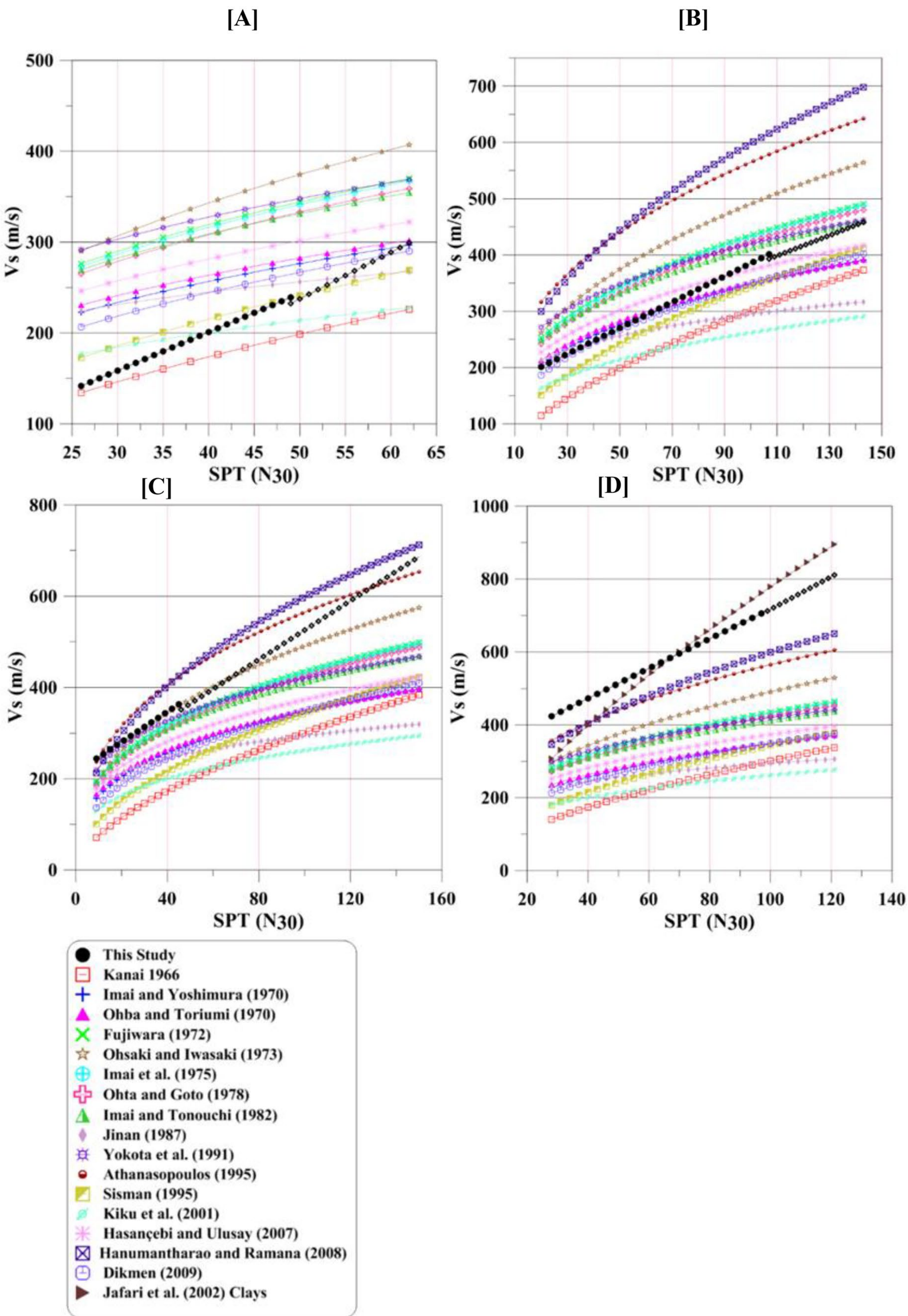
[A]
[B]
[C]
[D]
Vs (m/s)
SPT (N30)
This Study
Kanai 1966
Imai and Yoshimura (1970)
Ohba and Toriumi (1970)
Fujiwara (1972)
Ohsaki and Iwasaki (1973)
Imai et al. (1975)
Ohta and Goto (1978)
Imai and Tonouchi (1982)
Jinan (1987)
Yokota et al. (1991)
Athanasopoulos (1995)
Sisman (1995)
Kiku et al. (2001)
Hasançebi and Ulusay (2007)
Hanumantharao and Ramana (2008)
Dikmen (2009)
Jafari et al. (2002) Clays

Fig. 18 Microseismic zonation map for Egypt based on geological classification, NEHRP seismic site classification, and the refusal depth D50 (SPT(N_{30}) = 50 blows)

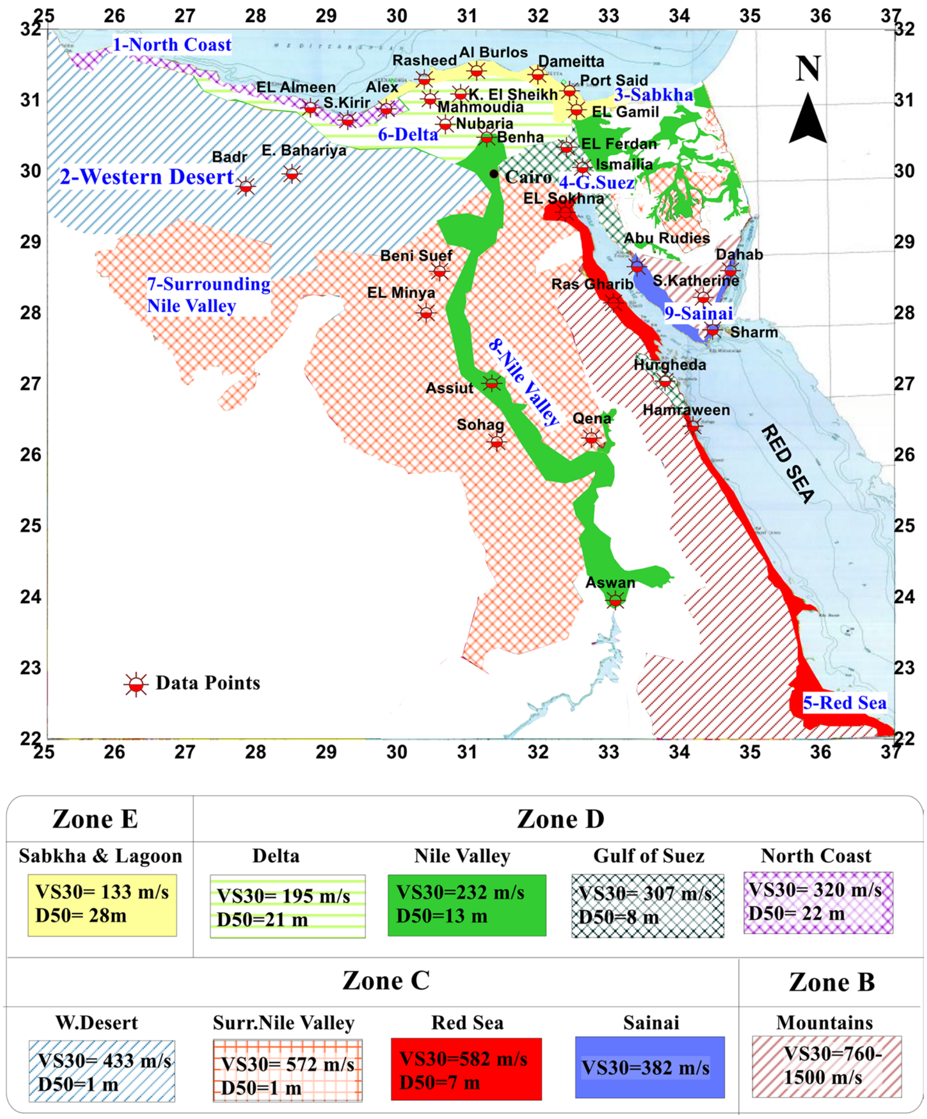

Table 4 The Egyptian soil NHRP classification and refusal depth values

Soil zone	Vs 30 (m/s)	Refusal depth D50	NHRP zone class
Sabkha and Lagoons	133	28	E
Delta	195	21	D
Nile Valley	232	13	D
Gulf of Suez	307	8	D
Northern Coast Soil	320	22	D
Sinai	382	——-	C
Western Desert	433	1	C
Surr. Nile Valley	572	1	C
Red Sea	582	7	C
Mountains	865	——-	B

Conclusions

A total of 71 drilling boreholes and about 82 V_s velocity tests varying between Downhole, Crosshole, ReMi, and MASW were used to prepare the microseismic zonation maps for Egypt. The geological map of Egypt was used to extrapolate the seismic and engineering data to determine 10 different geological zones, namely, (1) Sabkha and Lagoons, (2) The Delta, (3) The Nile Valley, (4) The Gulf of Suez, (5) The Northern Coast, (6) Sinai, (7) The Western Desert, (8) The Surrounding Nile Valley, (9) The Red Sea, and (10) The Mountains. The new empirical evidence for the V_s versus depth and SPT (N_{30}) versus depth that has been introduced by this study for each zone will help engineers and seismologists obtain the desired dynamic properties of the soil such as refusal depth (SPT (N_{30}) = 50 blows) or the dynamic shear modulus G.

This study introduced new relations for each geological zone between the V_s versus SPT (N_{30}) by solving equations of V_s 30 and SPT (N_{30}) with depth.

To the best of our knowledge, this microseismic zonation map is the first such map in Egypt that can be used to know about the value of V_s 30 and the NEHRP seismic zone class. This map will be very helpful for future projects in Egypt to evaluate the number of hazards that they projects might face.

This study has given important warnings based on the historical seismicity and NEHRP classification of certain seismic zones. In particular, warnings have been given to the three weak zones identified by this study, i.e., the sabkha and lagoons zone, the "Delta zone and the Capital Cairo," and the zone comprising the "villages of the Nile Valley." These zones have been found to be seismically weak for a long time and are suffering from weak NEHRP seismic zone classification ranging between Zone "E" to Zone D. These zones have many poor residents, and the people live in non-engineering constructions composed of old brick and wooden ceilings in areas such as "El Dowiqa." Any seismic activity can cause the ceiling to collapse, causing a huge loss of lives. A high risk has also been detected for future petroleum projects and oil rigs initiated in Idku and Rashid or in offshore Alexandria, where a wide destructive hazard may come from an offshore earthquake such as the earthquake of 1955 (M = 6.2). The reports regarding this historical earthquake have indicated that it had destroyed much of the construction and pipelines and caused many deaths in Idku and Rashid (Woodward and Clyde Consultant 1985).

Acknowledgements The authors would like to thank Prof. Dr. Arindam Basu, Editor-in-Chief, and the two capable reviewers for their keen interest, valuable comments on the manuscript, and improvements to enhance this work.

Availability of data and material The data are not available because of confidentiality.

Declarations

Conflicts of interest The authors declare no competing interests.

References

Akin MK, Kramer SL, Topal T (2011) Empirical correlations of shear wave velocity (Vs) and penetration resistance (SPT-N) for different soils in an earthquake-prone area (Erbaa-Turkey). Eng Geol 119:1–17

Andrus RD, Fairbanks CD, Zhang J, Camp WM III, Casey TJ, Cleary TJ, Wright WB (2006) Shear-wave velocity and seismic response of near-surface sediments in Charleston. South Carolina Bull Seismol Soc Amer 96(5):1897–1914

Andrus RD, Stokoe KH (1997) Liquefaction resistance based on shear wave velocity. In: Youd TL, Idriss IM (eds) NCEER Workshop on Evaluation of Liquefaction Resistance of Soils, Salt Lake City, UT, Technical Report NCEER-97-0022. National Center for Earthquake Engineering Research, Buffalo, NY, pp 89–128

ASTM Standards D1586–99 (1999) Standard test method for penetration test and split-barrel sampling of soils

ASTM Standards D4428 (2014) Standard test methods for crosshole seismic testing

ASTM Standards D7400 (2017) Standard test methods for downhole seismic testing

Athanasopoulos GA (1995) Empirical correlations Vs-N SPT for soils of Greece: a comparative study of reliability. In: Akmak ASÇ (ed) Proceedings of 7th International Conference on Soil Dynamics and Earthquake Engineering (Chania, Crete). Computational Mechanics, Southampton, pp 19–36

Ben-Menahem A (1979) Earthquake catalogue for the Middle East (92 B. C.–1980 A. D.). Boll Geofis Teor Appl 21(84):245–310

Ben-Menahem A, Aboodi E (1971) Tectonic patterns in the northern Red Sea region. J Geophys Res 76:2674–2689

Burland JB (1989) Small is beautiful: the stiffness of soils at small strains. Can Geotech J 26(4):499–516

Castelli F, Cavallaro A, Ferraro A, Grasso S, Lentini V, Massimino MR (2018) Static and dynamic properties of soils in Catania City (Italy). Ann Geophys 61(2):SE221. https://doi.org/10.4401/ag-7706

Cavallaro A, Capilleri PP, Grasso S (2018) Site characterization by dynamic in situ and laboratory tests for liquefaction potential evaluation during Emilia Romagna earthquake. Geosciences 8(7):242. https://doi.org/10.3390/geosciences8070242

Coccia S, Del Gaudio V, Venisti N, Wasowski J (2010) Application of Refraction Microtremor (ReMi) technique for determination of 1-D shear wave velocity in a landslide area. J Appl Geophys 71:71–89

Cochran JR (1983) A model for development of Red Sea. Bull Am Assoc Petrol Geol 67:41–60

Dikmen U (2009) Statistical correlations of shear wave velocity and penetration resistance for soils. J Geophys Eng 6:61–72

Dobry R, Borcherdt RD, Crouse CB, Idriss IM, Joyner WB, Martin GR, Power MS, Rinne EE, Seed RB (2000) New site coefficient and site classification system used in recent building code provisions. Earthq Spectra 16(1):41–67

EGSMA (Egyptian Geological Survey and Mining Authority) (1981) Geologic map of Egypt 1:2,000,000. EGSMA, Cairo

Freund R (1970) Plate tectonics of the Red Sea and east Africa. Nature 228:453

Fujiwara T (1972) Estimation of ground movements in actual destructive earthquakes. Proceedings of the Fourth European Symposium on Earthquake Engineering, London, pp 125–132

Gamal MA, Pullammanappallil S (2011) Validity of the Refraction Microtremors (ReMi) method for determining shear wave velocities for different soil types in Egypt. Int J Geosci 2:530–540

Girdler RW (1985) Problems concerning the oceanic lithosphere in northern Red Sea. Tectonics 116:109–122

Girdler RW, Styles P (1974) Two stages in the Red Sea floor spreading. Nature 247:7–11

Grasso S, Massimino MR, Sammito MSV (2021) New stress reduction factor for evaluating soil liquefaction in the coastal area of Catania (Italy). Geosciences 11(1):12. https://doi.org/10.3390/geosciences11010012

Grasso S, Maugeri M (2009) The seismic microzonation of the city of Catania (Italy) for the maximum expected scenario earthquake of January 11, 1693. Soil Dyn Earthq Eng 29:953–962

Grasso S, Maugeri M (2012) The seismic microzonation of the city of Catania (Italy) for the Etna scenario earthquake (M=6.2) of 20 February 1818. Earthq Spectra 28(2):573–594

Hanumantharao C, Ramana GV (2008) Dynamic soil properties for microzonation of Delhi. India J Earth Syst Sci 117(S2):719–730

Hasançebi N, Ulusay R (2007) Empirical correlations between shear wave velocity and penetration resistance for ground shaking assessments. Bull Eng Geol Environ 66:203–213
Holzer TL, Bennett MJ, Noce TE, Tinsley JC (2005) Shear-wave velocity of surficial geologic sediments in northern California: statistical distributions and depth dependence. Earthq Spectra 21:161–177
Idriss IM, Boulanger RW (2004) Semi-empirical procedures for evaluating liquefaction potential during earthquakes. Proceedings of the 11th IC SDEE/3rd ICEGE Proceedings, Berkeley, CA, USA, 1:32–56
Imai T (1977) P and S wave velocities of the ground in Japan. Proceeding of IX International Conference on Soil Mechanics and Foundation Engineering 2:127–132
Imai T, Fumoto H, Yokota K (1975) The relation of mechanical properties of soil to P- and S-wave velocities in Japan. Proceedings of 4th Japan Earthquake Engineering Symp. 89–96 (in Japanese)
Imai T, Tonouchi K (1982) Correlation of N-value with S-wave velocity and shear modulus. Proceedings of the 2nd European Symposium of Penetration Testing, Amsterdam, pp 57–72
Imai T, Yoshimura Y (1970) Elastic wave velocity and soil properties in soft soil. Tsuchi-ToKiso 18(1):17–22 (in Japanese)
Iyisan R (1996) Correlations between shear wave velocity and in-situ penetration test results. Chamber of Civil Engineers of Turkey. Tek Dergi 7(2):1187–1199 (in Turkish)
Jafari MK, Asghari A, Rahmani I (1997) Empirical correlation between shear wave velocity (Vs) and SPT-N value for south of Tehran soils. Proceedings of 4th International Conference on Civil Engineering (Tehran, Iran) (in Persian)
Jafari MK, Shafiee A, Razmkhah A (2002) Dynamic properties of fine grained soils in south of Tehran. J Seismol Earthqu Eng 4:25–35
Jinan Z (1987) Correlation between seismic wave velocity and the number of blow of SPT and depth. Selected Papers from the Chinese. J Geotech Eng 92–100
Kanai K (1966) Conf. on Cone Penetrometer. The Ministry of Public Works and Settlement (Ankara, Turkey) (presented by Y Sakai, 1968)
Kanlı AI, Tildy P, Prónay Z, Pınar A, Hermann L (2006) Vs 30 mapping and soil classification for seismic site effect evaluation in Dinar region, SW Turkey. Geophys J Int 165:223–235
Kayabalı K (1996) Soil liquefaction evaluation using shear wave velocity. Eng Geol 44(1):121–127
Kebeasy RM (1990) Seismicity. In: Said R (ed) Geology of Egypt. Rotterdam, Brookfield: A. A. Balkema, pp 51–59
Kiku H, Yoshida N, Yasuda S, Irisawa T, Nakazawa H, Shimizu Y, Ansal A, Erkan A (2001) In-situ penetration tests and soil profiling in Adapazari, Turkey. Proceedings of the ICSMGE/TC4 Satellite Conference on Lessons Learned From Recent Strong Earthquakes, pp 259–265
Kramer SL (1996) Geotechnical Earthquake Engineering. Prentice Hall, Upper Saddle River, New Jersey
Lee SH (1990) Regression models of shear wave velocities. J Chin Inst Eng 13:519–532
Lehane B, Fahey M (2002) A simplified non-linear settlement prediction model for foundations on sand. Can Geotech J 39(2):293–303
Louie JN (2001) Faster, better: shear-wave velocity to 100 meters depth from refraction microtremors arrays. Bull Seismol Soc Amer 91(2):347–364
Maamoun M, Megehed A, Allam A (1984) Seismicity of Egypt, Bull. Helwan Inst Astro Geophys IV, Ser B:109–160
Makropoulos KC, Burton PW (1981) A catalogue of seismicity in Greece and adjacent areas. Geophys J R Astr Soc 65:741–762
Mayne PW, Schneider JA, Martin GK (1999) Small- and large strain soil properties from seismic flat dilatometer tests. Proceedings of 2nd Int Symp on Pre-Failure Deformation Characteristics of Geomaterials, Torino, 1, pp 419–427
McGillivray AV (2007) Enhanced integration of shear wave velocity profiling in direct push site characterization systems. Ph.D. thesis, Georgia Institute of Technology, 370 pp
McGillivray AV, Mayne PW (2004) Seismic piezocone and seismic flat dilatometer tests at Treporti. Proceedings of 2nd Int. Conf. on Site Characterization, Porto, 2, pp 1695–1700
McKenzie DP (1972) Active tectonics of the Mediterranean region. Geophys J Roy Astronom Soc 30:109–185
Meshref WM (1990) Tectonic framework. In: Said, R. (ed) Geology of Egypt. Rotterdam, Brookfield: A. A. Balkema, pp 113–156
Miller RD, Park CB, Ivanov JM, Xia J, Laflen DR, Gratton C (2000) MASW to investigate anomalous near-surface materials at the Indian refinery in Lawrenceville. Kansas Geology Survey, Open-File Report, Lawrence, p 48
Neev D, Hall K, Saul JM (1982) The Pelusim megashear system across Africa and associated lineament swarms. J Geophys Res 87:1015–1030
NEHRP (National Earthquake Hazards Reduction Program) (2007) Program overview. Available at www.nehrp.gov/pdf/nehrp_acehr_ppt.pdf. Accessed 26 October 2020
NEIC and USGS (1964-2020) National Earthquake Data Centers, Preliminary determination of epicenters, monthly listing, U.S Department of the interior/ Geological survey, National Earthquake information center and USGS Preliminary Determination of Epicenters (PDE) Bulletin https://earthquake.usgs.gov/data/pde.php
Ohba S, Toriumi I (1970) Dynamic response characteristics of Osaka Plain. Proceedings of the Annual Meeting, A. I. J (in Japanese)
Ohsaki Y, Iwasaki R (1973) On dynamic shear moduli and Poisson's ratio of soil deposits. Soils Found 13:61–73
Ohta Y, Goto N (1978) Empirical shear wave velocity equations in terms of characteristics soil indexes. Earthq Eng Struct Dyn 6:167–187
Papazachos BC, Comninakis PE (1971) Geophysical and tectonic features of the Aegean arc. Geophys Res 76:8517–8533
Papazachos BC, Papaioannou ChA, Margaris BN, Theodulidis NP (1993) Regionalization of seismic hazard in Greece based on seismic sources. Nat Hazards 8:1–18
Park CB, Miller RD, Xia J (1999) Multi-channel analysis of surface waves. Geophysics 64(3):800–808
Pitilakis K, Raptakis D, Lontzetidis KT, Vassilikou T, Jongmans D (1999) Geotechnical and geophysical description of Euro-Seistests, using field and laboratory tests, and moderate strong ground motions. J Earthqu Eng 3:381–409
Pullammanappallil S, Honjas B, Louie J, Siemens JA, Miura H (2003) Comparative study of the refraction microtremors method: using seismic noise and standard P-wave refraction equipment for deriving 1D shear-wave profiles. Proceedings of the 6th SEGJ International Symposium, Tokyo, January 2003, pp 192–197
Quennell AM (1984) The western Arabian rift system. In: Dixon JE, Robertson AHF (eds) The geological evolution of the eastern Mediterranean. Publishers Oxford, Blackwell Scientific, pp 75–788
Riad S, Meyers H (1985) Earthquake catalog for the Middle East countries 1900–1983. World Data Center for Solid Earth Geophysics, Rep. SE-40. National Oceanic and Atmospheric Administration (NOAA), US Department of Commerce, Boulder, Colorado, USA
Richart FE, Hall JR, Woods RD (1970) Vibrations of soils and foundations. Prentice-Hall Inc, New Jersey
Sasitharan S, Robertson PK, Sego DC, Morgenstern NR (1994) State-boundary surface for very loose sand and its practical implications. Can Geotech J 31:321–334
Schnabel PB, Lysmer JL, Seed HB (1972) SHAKE: a computer program for earthquake response analysis of horizontally layered sites. Report EERC-72/12, Earthquake Engineering Research Center (EERC), Berkeley, California

Seed HB, Idriss IM (1970) Soil moduli and damping factors for dynamic response analyses. Rep. No. EERC-70/10, Earthquake Eng. Research Center, Univ. of California at Berkeley, Berkeley, California

Seed HB, Idriss IM (1981) Evaluation of liquefaction potential sand deposits based on observation of performance in previous earthquakes. ASCE National Convention (MO), pp 481–544

Seed RB, Cetin KO, Moss RES, Kammerer AM, Wu J, Pestana JM, Riemer MF, Sancio RB, Bray JD, Kayen RE, Faris A (2003) Recent advances in soil liquefaction engineering: a unified and consistent framework. 26th Annual ASCE Los Angeles Geotechnical Spring Seminar, Long Beach, CA, ASCE, Reston, VA, 71

Shapira A (1994) Seismological Bulletin of Israel, pp 1900–1994

Shibuya S, Yamashita S, Mitachi T, Tanaka H (1995) Effects of sample disturbance on G_{max} of soils—a case study. 1st International Conference on Earthquake Geotechnical Engineering, Tokyo, Japan, 1, pp 77

Sisman H (1995) An investigation on relationships between shear wave velocity, and SPT and pressuremeter test results. MSc Thesis, Ankara University, Geophysical Engineering Department, Ankara, p 75 (in Turkish)

Stewart JP, Liu AH, Choi Y (2003) Amplification factors for spectral acceleration in tectonically active regions. Bull Seismol Soc Amer 93(1):332–352

Strobbia C, Boaga J, Cassiani G (2015) Double-array refraction microtremors. J Appl Geophys 121:31–41

Sykora DE, Stokoe KH (1983) Correlations of in-situ measurements in sands of shear wave velocity. Soil Dyn Earthq Eng 20:125–136

Walter DM (1981) IASPEI Workshop: seismic modeling of laterally varying structures. EOS Trans Am Geophys Union 62(2):18–19

Wills CJ, Silva W (1998) Shear wave velocity characteristics of geologic units in California. Earthq Spectra 14(3):533–556

Woodword Clyde Consultant WWCC (1985) Earthquake activity and dam stability for the Aswan High Dam, Egypt. High and Aswan Dames Ministry of Irrigation, Cairo 2

Yokota K, Imai T, Konno M (1991) Dynamic deformation characteristics of soils determined by laboratory tests. OYO Tee Rep 3:13